Calibration and validation of the Dynamic Photorefraction system (DPRS)

by

Vivek Labhishetty

A thesis
presented to the University of Waterloo
in fulfillment of the
thesis requirement for the degree of
Master of Science
in
Vision Science

Waterloo, Ontario, Canada, 2014

AUTHOR'S DECLARATION

I hereby declare that I am the sole author of this thesis. This is a true copy of the thesis, including any required final revisions, as accepted by my examiners.

I understand that my thesis may be made electronically available to the public.

Abstract

Introduction

Our group has been measuring accommodation in myopic children. The instrument of choice has been the Power Refractor (Multichannel Systems). However, this instrumentation is no longer supported and runs on an outdated platform (Windows 98). There is a need to develop a new photorefraction system that has the ability of the Power Refractor to accurately measure accommodation dynamically. The resolution of measures can be increased with modern video cameras especially in regards to the measurement of the first and second order dynamics of the accommodative response.

Photorefraction is a rapid video based means to measure the refractive status of the eye. Light from infra-red LEDs set eccentric to the aperture of the camera is reflected back from the eye forming intensity gradients across the pupil that varies with the degree of ocular defocus relative to camera. However, this gradient can be influenced by various factors such as pupil size, fundus brightness etc. Thus the relationship between defocus and the intensity gradient must be calibrated empirically in order that valid measures of accommodation can be made from the photorefractor. Calibration trials determine a *conversion factor* which will be used to convert intensity gradients into diopters where other optical parameters such as pupil brightness and pupil size are controlled. Furthermore, once designed, this new instrument should be validated to see if it can accurately measure the ocular accommodative response and its dynamic characteristics.

Methods

Two calibration procedures were employed for conversion of the luminance slope in to units of diopters. First being the relative calibration where relative changes in the accommodation were induced and was related to the absolute changes showed in the luminance slope output from the photorefractor. Second, pupil size calibration was done to account for the changes in the pupil size where the conversion factor obtained from each subject was related to their respective luminance measure across the pupil (fundal brightness). For relative calibration, varying degree of ocular focus ranging from +5D to -5D (1D steps) was induced using trial lenses in-front of the right eye in which visible light was filtered out using an infra-red filter. Subjects (20-40 yrs.) fixated at a distance target with the other eye. Intensity gradients obtained in each condition were then plotted against the induced lens to get the linear regression slope value (conversion factor). This conversion factor was used later to convert the luminance output given by the photorefractor in to diopters. Repeatability measures were taken on 4 subjects (20-40 yrs.) on a different day. Bland-Altman plots were used to test the repeatability of conversion factor between the two visits. To address the inter-individual variability of the conversion factor, pupil size calibration was employed wherein fundus brightness was plotted against conversion factor and the linear regression equation of this plot was used to calculate the conversion factor. This procedure was used to account for changes in the pupil size during an accommodative response and thus to enhance the accuracy of the estimation.

For validation, accommodation was stimulated using high contrast vertical line targets placed in a Badal optical system. A 2D step was provided with a 4sec presentation time and the onset of the stimulus was randomized. The video output obtained was loaded into DPRS for

analysis. The raw position data obtained was further loaded in to MATLAB for analyzing the dynamics characteristics of the response using the velocity threshold criterion.

Results

Calibration slopes of 12 subjects (29.16 ± 3.13 years) ranged from 1.77 to 3.41. Mean (±SD) slope obtained was 2.86±0.46. Bland-Altman plots showed a good repeatability of the conversion factor calculation between the visits for the four subjects (30.75 ± 4.11 years) with a coefficient of repeatability (Mean+1.96SD) of the slope values was 0.20 (≈0.05D). Fundus brightness showed a negative correlation with the calculated conversion factor across the subjects and then linear regression (y = -0.008x + 2.66; R^2 = 0.73) was used to calculate the conversion factor.

Validation was performed on 9 subjects (7 adults (29.57±2.69 years) and 2 children (11±1.4 years)). Conversion factors were obtained from all the subjects and it ranged from 1.48 to 2.08. Four out of nine subjects showed sluggish accommodative responses with an accommodative gain value less than 0.5. Bland-Altman plots showed good agreement between the DPRS (both individual and pupil size calibration) and the dynamic retinoscopy (mean deviation of 0.16D and 0.24D respectively). Individual calibration was slightly more accurate than the pupil size calibration and a mean deviation of 0.06D was noted between the two methods for estimating the defocus using the calculated conversion factors.

Discussion

A new dynamic photorefraction along with an offline dynamic photorefraction system (DPRS) was calibrated and validated. Modifications done during this process made the system more robust with a linear operating range for a dioptric range of +5D to -5D. Photorefraction

measures showed significant inter-individual variability in conversion factors as suggested previously (Schaeffel et al., 1993) with a good repeatability. In order to address the pupil size variability during a dynamic accommodative response and inter-individual variability of the conversion factors, the fundus brightness of the subjects were plotted against their respective conversion factors. The linear regression (y = -0.008x + 2.66; R^2 = 0.73) was used to calculate the conversion factors directly from the fundal brightness. This procedure not only accounted for changes in the pupil size but also for calculation of conversion factors directly. Further, the system was validated on nine subjects and the responses obtained were in agreement with the previous literature on accommodation dynamics (Campbell et al., 1960; Tucker et al., 1979; Suryakumar et al., 2005). Bland-Altman plots showed agreement between the DPRS and the gold standard dynamic retinoscopy with a clinically insignificant mean deviation in the accommodative gain estimation between the methods.

Acknowledgements

I would like to take this opportunity to sincerely thank each and every one here at Waterloo for their support and warmth, making these two years a memorable experience.

I owe my deepest gratitude to my supervisor, mentor and project guide Dr.William R Bobier for his never ending support and guidance right from the beginning of my Masters be it conceptualization, instrumentation, experimental design, or even trouble shooting of the problems encountered.

I want to sincerely thank my committee members, Dr.Trefford Simpson and Dr.Vasudevan Lakshminarayanan, for their exemplary guidance, cordial support and a constant encouragement throughout the course of my Masters.

I would also like to thank my lab mates Dr.Raiju J Babu and Rajkumar N Raveendran for all the support and encouragement they gave me when I had tough times figuring out issues related to the instrumentation and experimental design. A special thanks to Varadharajan Jayakumar for his valuable technical guidance and support during this course. Further, I want to thank Amy Chow, summer student at our lab for helping me out in the analysis of my data.

I would like to thank all my course instructors (Dr.Irving, Dr.Bobier, Dr.Vengu, Dr.Simpson and Dr.Hutchings) for their academic guidance. I would also like to thank Andrew for his technical support in building the experimental design. Further, I would like to thank Derek Kwok, Rajaraman Suryakumar for their help with the DPRS.

A whole hearted thanks to all my fellow graduate students for showing endurance and supporting me by participating in the various instrument related modifications done during

this course. This project wouldn't be possible without your support. Also, I want to thank GIVS for organizing all the amazing grad events and the mouth-watering BBQ.

A heart-felt thanks to the so called Indian gang (Krithika and Raiju, Sruthi and Lakshman, Jaya and Jeevan, Kalpana and Prem, Dr.Jalaiah, Varadhu, Raj and Amith) here at Waterloo for bearing me for two long years.

Lastly, I want to thank University of Waterloo for giving me this platform to explore myself. Without this opportunity, doing Masters and PhD would have been a distant dream for me.

Dedication

To dad, mom, brother and family for their humongous love and support

Table of Contents

List of Figures

List of Tables

Chapter 1. Eccentric photorefraction

1.1   Introduction

Eccentric photorefraction is a quick and accurate video-based objective technique used for measuring the refractive status and accommodation of the eye (Bobier et al., 1985; Schaeffel et al., 1987 and 1993). Bobier and Braddick (1985) coined the term "Eccentric photorefraction" as the technique was performed with its source placed in an offset/ eccentric position to the center of the camera aperture. Eccentric photorefraction was based on the idea of 'Static photographic skiascopy' which was used as a screening tool in the late '70s (Kaakinen, 1979 and 1981; Howland, 1980). Eccentric photorefraction works on a principle similar to retinoscopy (Roorda et al., 1995). As shown in Figure 1-1, in eccentric photorefraction, light from LEDs placed at various eccentricities is sent into the eye. A smaller proportion of this light is reflected back from the eye. Reflex crescents formed by each eccentric source ultimately superimpose to produce a linear intensity distribution pattern across the pupil (Schaeffel et al., 1987, 1993). The early photographic measures using the camera film was based on the idea that with a single eccentric source, the extent of crescent of light across the pupil varies with the type and degree of refractive error over a limited working range (Bobier, 1985; Howland, 1985). A modification was later presented with video-based systems having sources at multiple eccentricities to increase the working range (Schaeffel et al, 1986). Furthermore, empirical investigations (Schaeffel et al., 1993) showed that the slope of the intensity distribution across the pupil (instead of crescent extent) varied linearly with defocus (again within a limited working range) and is a better indicator of the defocus. These

empirical findings were later supported by Roorda et al. (1997) using optical ray tracing technique.

Because of the ability to take rapid measurements, photorefraction has been widely used in vision screenings and research studies involving infants, who have shorter attention spans or poor cooperation (Choi et al., 2000). The commercial development of the Power Refractor has allowed photorefraction become one of the commonly-used instruments to measure the dynamic characteristics of accommodative response given its remote working distance and its superior sampling rate (Howland, 2009) compared to autorefractors.
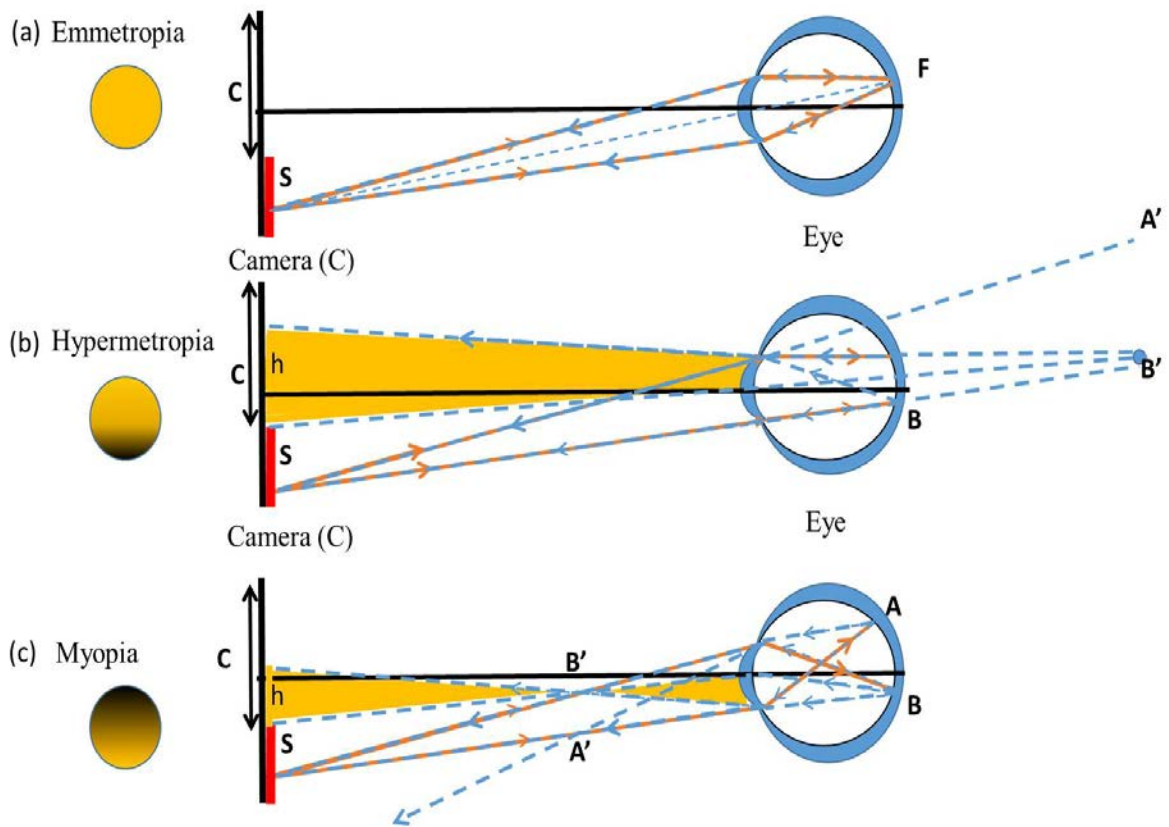
Figure 1-1: Optics of the Eccentric photorefraction.

Patterns of light within the pupil vary based upon the eye's focus defocus with respect to the camera. This can be explained by identifying the waist of rays (h) entering the camera from a single led from the extended source. Light (extreme ray) from the infra-red (IR) light emitting diodes (LEDs), denoted by S,

placed at multiple eccentricities (below) from the center of the camera aperture is sent into the eye (represented by the orange solid line). Depending on the dioptric focus of the eye in relation to the camera, the slope of the intensity distribution of the reflected light varies across the pupil. (a) If the eye is focused on the camera, light focused on the retina (F) when reflected back (blue dotted lines) will re-focus on to LEDs(S). An eye in focus with the source without any aberrations will result in a dark pupil. When the eye is defocussed either in-front or behind the led sources, crescents of light are formed in the pupil which vary in direction and slope depending upon the degree and direction of defocus. (b) In case of a hyperopic defocus in relation to the camera, the incident light (orange solid line) will be focused behind the retina forming a blurred image AB on the retina. A virtual image A'B' is formed at the plane of the far point (denoted by blue dotted line) behind the eye. If the eye is hyperopic, the reflected light will focus at a far point behind the camera. Since the lower half of the camera is covered by the LED sources, rays (height h) only from the upper half of the retina (yellow shade) will reach the camera sensor. (c) Similarly, in case of myopia, rays (orange solid line) focus in-front of the retina (blur circle AB). An inverted aerial image B'A' (blue dotted lines) is formed at the far point of the subject. In case of a myopic defocus in relation to the camera, the reflected light focuses in-front of the retina due to which only rays from the lower half of the pupil (yellow shade) will reach the camera of height h [adapted from Bobier and Braddick, 1985].

Empirical studies (Bobier et al., 1985; Schaeffel et al., 1987, 1993) and optical investigations Roorda et al., 1995, 1997) agreed that the arrangement of the LEDs produce a linear intensity distribution pattern across the respective meridian of the pupil that varies in the height and extent with the amount and type of defocus (refer Figure 1-1 for optics of PR). This relationship however is limited to a specific working range. Other than defocus, the direction and size of the crescent of light visible within the pupil is also dependent on optical (pupil diameter, fundus brightness, aberrations) and non-optical (working distance, camera limiting aperture and eccentricities of the source) factors (Howland, 1985; Bobier WR et al., 1985; Roorda et al., 1997). Theoretical (Roorda et al., 1995 and 1997) and empirical studies (Schaeffel et al., 1993 and 1994) provide a supportive evidence for the impact of these optical and non-optical parameters on the gradient of light intensity across the pupil. Since the photorefraction analysis software gives out the slopes of intensity distribution across the pupil, to estimate the degree of defocus, a calibration function (conversion factor) that converts the steepness of the intensity distribution across the pupil into units of diopters needs to be calculated. Bobier et al. (1985) showed that accurate measures of refractive error and accommodation can be obtained only when the photorefractive output is interpreted in terms

of calibration obtained from the eye with known refractive defocus. A similar calibration procedure was applied later (Schaeffel et al., 1993) for changes in the slope of intensity distribution across the pupil when known refractive defocus was induced.

Optical analysis (Bobier et al, 1985; Roorda et al., 1997) and empirical data (Schaeffel, 1987, 1993) have described the optics of slope patterns across the pupil in terms of four key optical parameters, (a) refractive state, (b) pupil diameter, (c) the eccentricity of the source and (d) the camera to subject working distance. For our purposes we are interested in linking refractive error (or accommodative state) to the slope pattern and controlling the influence of the other variables.

1.1.1 Critical optical parameters

1.1.1.1 Pupil diameter
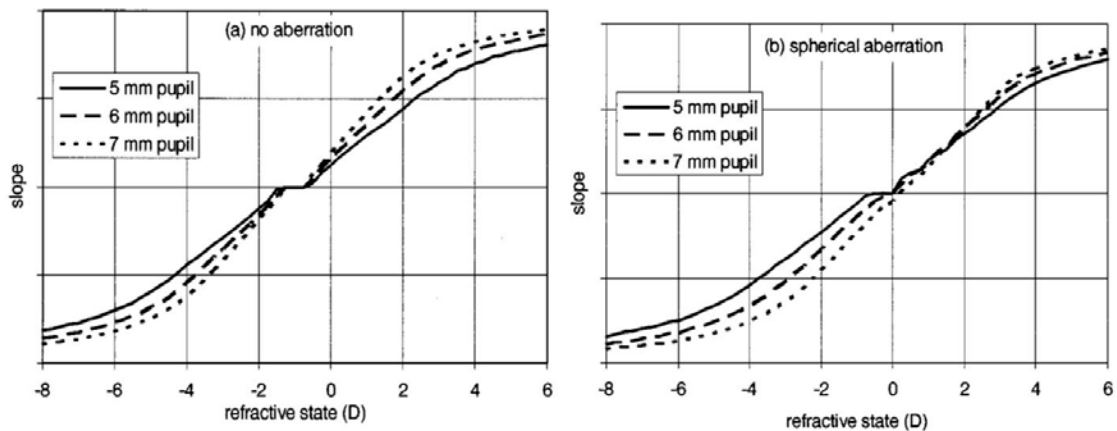
Figure 1-2: Luminance slope output is shown as a function of the refractive state (D) at various pupil sizes.

The gain (derivative of the slope as a function of refractive state) has been shown to increase with increasing pupil size. Furthermore, the point of saturation occurs at lower defocus levels with larger pupils. With the presence of spherical aberration, it is shown to shift the curve towards hyperopia. Further, the dead zone uncertainty of the instrument (i.e. refractive change in which a change in the linear intensity distribution is not seen) is shown to decrease in eyes with spherical aberrations and larger pupil size. This picture has been taken from the paper by Roorda et al. (1997) and copyright permission was obtained (The Optical society of America; Appendix C).

4

Figure 1-2 shows that the larger the pupil size, the larger the slope values for a particular

defocus with an early saturation (i.e. saturation at lower defocus). Roorda et al. (1997) has

shown in theory that refractive state estimation errors of over 1D can occur when calibration

functions measured at 5mm pupil were applied to one with 7mm pupil. Studies have

suggested that accurate photorefraction is possible only when the calibration functions

account for a varying pupil size (Bobier et al., 1985; Schaeffel et al., 1993; Roorda et al.,

1997).

1.1.1.2 Eccentricity and working distance

The eccentricity of the light source and the working distance affect the sensitivity of the

photorefractor (Figure 1-3). At a particular working distance, with an increase in the

eccentricity of the source, the dead zone uncertainty of the instrument increases allowing only

higher refractive defocus estimations (i.e. shifting the operating range).
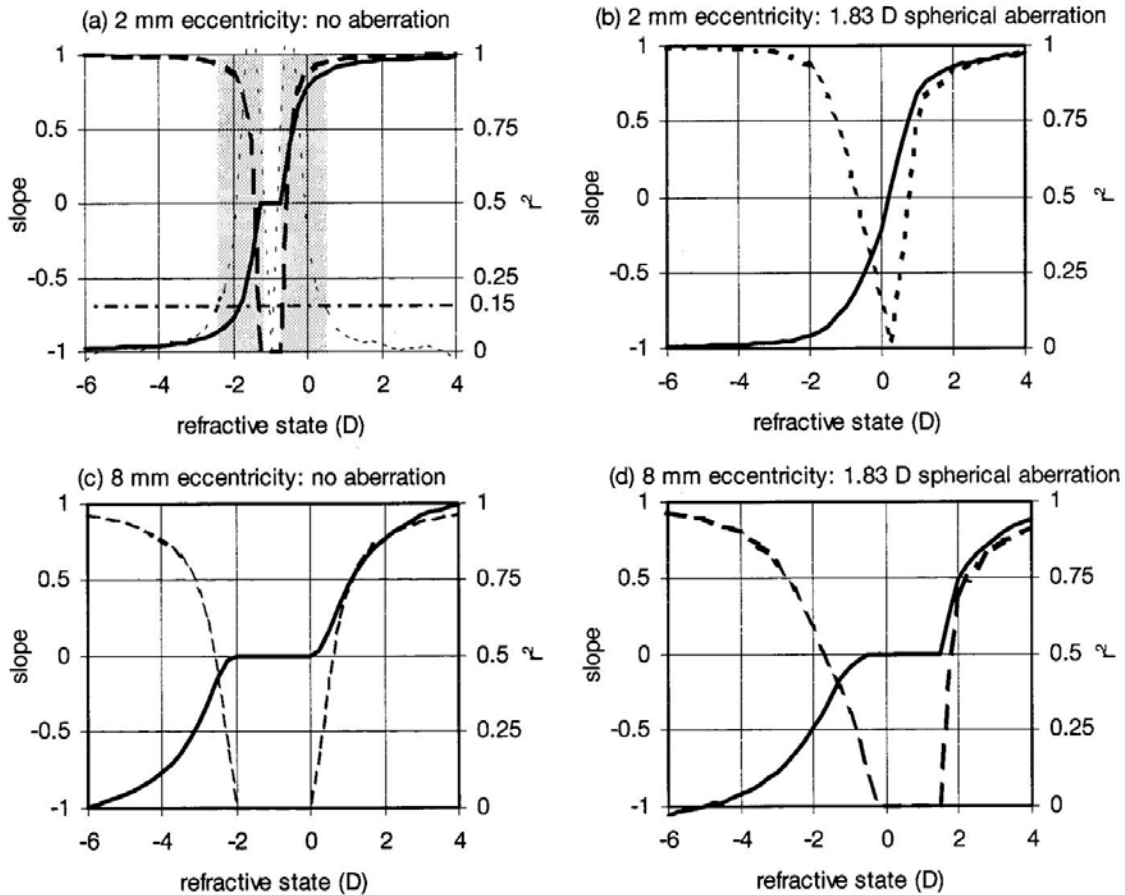
Figure 1-3: Plots of luminance slope outputs as a function of the refractive state with sources at various eccentricities.

The solid curve represents the slope of the intensity profile across the induced refractive defocus. The heavy dashed lines indicate the R^2 value for slope fitted to the calculated intensity profile. (a) The light dashed lines indicate the gain while the shaded area indicates the working range. As shown at 2mm eccentricity (a), (b), the dead zone uncertainty is small with an early saturation and smaller working range. But with a source at 8mm eccentricity, although the dead zone increases, the point of saturation occurs at a higher refractive state with a larger working range. This picture has been taken from the paper by Roorda et al. (1997) after obtaining copyright permission (The Optical society of America; Appendix C).

Furthermore, as shown in the figure 1-3, the rate of change of the slope of intensity profile with defocus and the slope value at a particular defocus decreases with an increase in the eccentricity of the source. Empirical evidence from Schaeffel et al. (1993) have provided support to these predictions on the impact of the working distance and eccentricity on the operating range of the photorefraction. Empirical evidences (Schaeffel et al., 1987, 1993)

6

have also suggested that with multiple eccentricities, ideal operating span is achieved over a range of defocus away from the camera and prior to saturation.

1.1.1.3 Other factors

Other factors such as eye-camera alignment, camera limiting aperture, equipment design, retinal reflectance, photoreceptor properties etc. (Howland, 1985; Bobier et al., 1985; Schaeffel et al., 1994; Bharadwaj et al., 2013) were shown to influence the slope of the intensity profile as a function of the induced refractive defocus.

Successful photorefraction can be achieved only when the luminance output is converted accurately into defocus measures (i.e. units of diopters). This can be done by calibrating each individual to get a conversion factor that is used for converting luminous units into diopters. A typical calibration trial involves calculating slopes of the luminous distribution across the pupil when known magnitude of defocus (Both hyperopia and myopia) is induced by adding a series of lenses before an eye when visible light is filtered out using an IR filter. The slope values obtained is then plotted against the induced refractive error (i.e. induced lens) to calculate the conversion factor (calibration function). The conversion factor for a particular individual is normally repeatable with low intra-subject variability, but was shown to have a high inter-subject variability (Schaeffel, 1993).

1.1.2 Photorefraction limitations

One of the major drawbacks of the photorefraction technique is the need to calibrate each individual to obtain an accurate estimation of the refractive error or defocus. This has to be done to account for the individual variances in the optical characteristics (Bobier et al., 1985; Schaeffel et al., 1993). The measurement of the slope of the intensity profile across the pupil

7

is limited to a specific working range depending on the eccentricity of the source and the working distance (Roorda et al., 1997). Also, empirical calibrations should account for the pupil size effects on the intensity profiles.

1.2 Purpose and rationale

The findings of a reduced accommodative response, elevated AC/A (Gwaizda, 1999; Mutti, 2000) coupled with a high degree of accommodative adaptation (Jiang, 1999) in children with myopia do not follow the expected patterns predicted by the existing models of accommodation and vergence (Schor, 1986) which suggest an inverse relationship between the cross-links and adaptive mechanisms. One explanation for a high accommodative adaptation could be resultant from a slower velocity of accommodation in myopes. This hypothesis is based upon empirical investigations (Schor and Kotulak, 1986) showing that higher levels of accommodative adaption are found when the frequency of reflex input is low and conversely high velocity of reflex accommodation attenuates accommodative adaptation. Accordingly, measuring the dynamics of accommodation in young myopes within the ages of 7 to 15 years showing high levels of AC/A ratio (Gwaizda, 1999) and accommodative adaptation (Jiang, 1999) can provide an insight about the sluggishness of the accommodative mechanism in myopia. A high speed photorefractor is an ideal option to measure the dynamics of accommodation in myopic children.

1.2.1 The need for further development

Though the currently available photorefractors (like Power Refractor, Multichannel Systems, Germany) are commonly used as either screening tools (Choi, 2000) or for research purposes (Blade, 2006), there is a need to develop a newer photorefraction system due to certain

technical limitations of the current photorefraction systems. A major limitation is that these photorefractors work on Windows 98 platform which is outdated and no longer technically supported. The Power refractor is based on an average estimation with no option of individual calibration to account for variation in the optical characteristics. This estimation might reduce the accuracy of refractive error estimation. Also considering its lower sampling frequency (25Hz), estimation of the first and second order dynamics is limited. Suryakumar et al. (2005) have shown that accommodative peak velocity and acceleration traces are smoothened and underestimated when measured at a sampling rate of 25Hz compared to 75Hz (Figure 1-4).
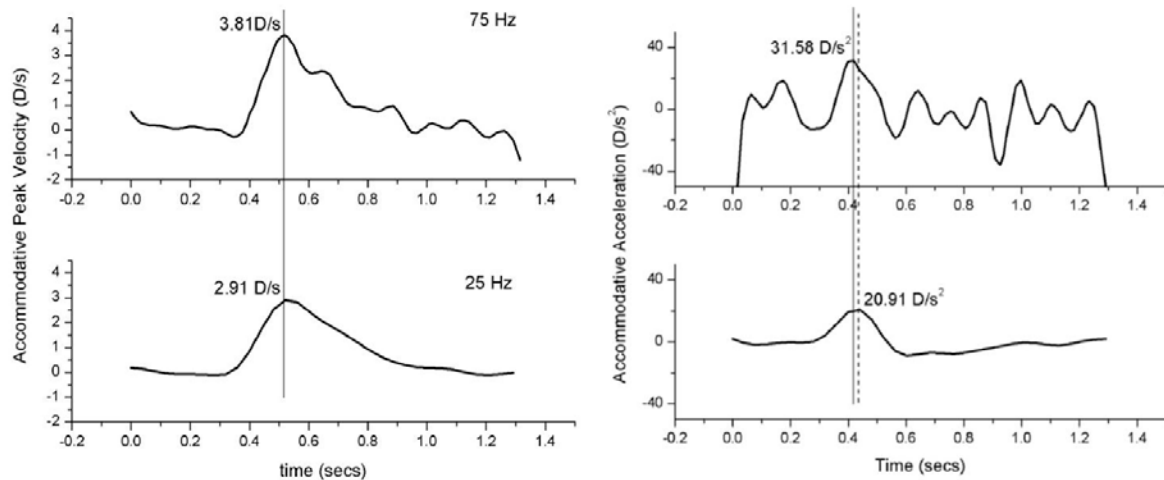
Figure 1-4: Velocity and acceleration profiles of the accommodation over time (top: 75Hz; below: 25Hz).

(a)Velocity traces measured at 25Hz appeared to be underestimated (2.91D/s over 3.81D/s) and smoother compared to the trace measured at 75Hz. (b) Further, acceleration traces measured at 25 Hz showed a larger underestimation (20.91D/s^2 over 31.58D/s^2) with a smooth trace. This picture was taken from Suryakumar, 2005. (Copyright obtained the author – Suryakumar (Appendix D)).

A newer system that works with modern interface a higher sampling frequency needs to be designed. Furthermore, this system should provide an option of individual calibration to enhance the accuracy of the dioptric estimation of defocus.

1.3   Dynamic photorefractor design

Accordingly, a new video-based eccentric photorefractor with a higher sampling frequency (70 Hz) was designed at our lab (Suryakumar et al., 2009). The configuration of this new eccentric photorefractor is based on the design used by Schaeffel et al. (1987). As shown in figure 1-5, it is a fire-wire charge coupled device (CCD) camera (PROSILICA CAM (EC750), Allied Vision Technologies, Canada) with infra-red (IR) light emitting diodes (LEDs) set at the knife-edge covering the lower half of the camera. Multiple eccentricities have been incorporated to extend the range of measurement and its precision (Schaeffel et al., 1993; Roorda et al., 1995).

Figure 1-5: Dynamic photorefractor.

(a) It is a Fire-wire charge coupled device (CCD) camera (PROSILICA CAM (EC750), Allied Vision Technologies, Canada) with infra-red (IR) light emitting diodes (LEDs) set at the knife-edge covering the lower half of the camera. (b) A total of 44 LEDs arranged in 8 rows with a maximum eccentricity of 45mm

are mounted on an aluminium plate and then fixed onto the camera. Peak wavelength of the LED source used is 895nm.

Since we were interested only in accommodative measurements, a single meridian was chosen to measure gradient profile. While power-refractor measures multiple meridians in order to compute the sphere and cylinder components of refractive error, the measures of dynamic accommodation is taken similarly from a single vertical meridian. Vertical meridian across the pupil was chosen for measurement of defocus (accommodation) and the LEDs are arranged accordingly. Empirical calibrations with this design have shown to provide a linear change in the intensity distribution over a range of defocus (±4D) with a small dead zone uncertainty (Suryakumar et al., 2007).

1.3.1 Dynamic photorefraction system (DPRS)

Key to the current photorefraction systems is the underlying analysis software which upon receiving the video information of intensity patterns across the pupil, converts it into defocus (refractive error or accommodative) measures along the vertical meridian. Accordingly, a novel analysis algorithm was designed, the Dynamic Photorefraction System (DPRS). It is a robust offline application that allows a rapid and a standardized estimation of the pupil size and accommodation. All the components involved in this algorithm have been described elsewhere (Suryakumar et al., 2009).
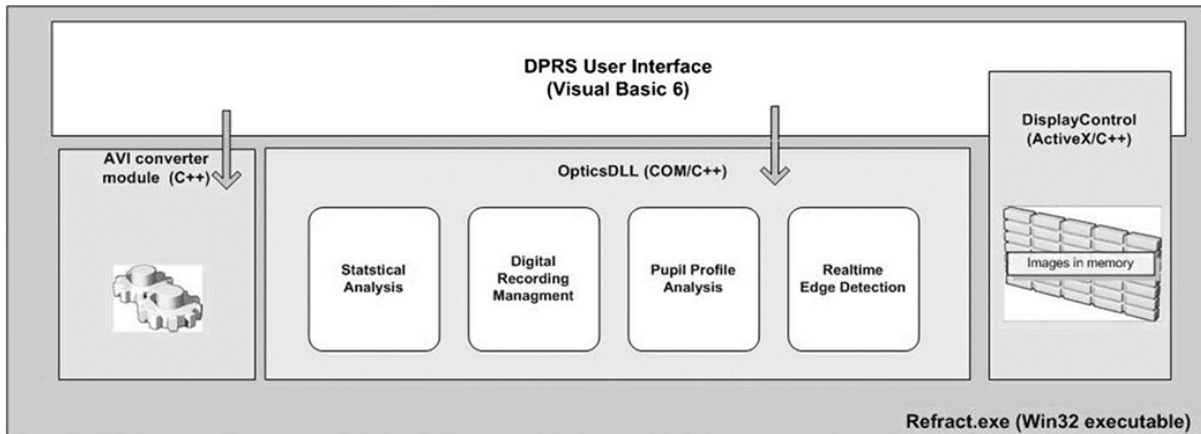
Figure 1-6: An illustration of the algorithm.

First, the recording of the photorefractor would be converted into a video file (.avi format) by the AVI module to access individual frames. Second, the frames would be read by the Optics DLL module, where edge detection, pupil determination and gradient profile estimation along the vertical meridian would be processed. Finally, the individual frames would be played back by the display control component. All the components were run as a Win32 executable (Refract.exe). The image has been taken from Suryakumar et al, 2009 (Copyright permission obtained from Elsevier; Appendix B).

The AVI output from the video recording software would be converted by the AVI module such that individual frames of the output could be accessed. These frames were then processed to detect and define the edge of the pupil. It would be an iterative process which involves edge detection by looking at the intensity difference between the neighboring pixels. If the identified pixels were above the pre-set threshold value, then they were considered as edge points. Often high reflective noise and/ or central corneal Purkinge reflection were mistaken as edge points. Therefore two post-processing steps have been incorporated to address these issues with both the steps involve finding any four-neighbor connected components of the approximated edge pixels. Firstly, if these connected components consist of too few (< 3) pixels, it was considered as a noise component and removed. Secondly, if the ratio of the number of pixels within the area of the bounding rectangle of the component exceeded a predefined threshold, it was considered as a reflection and discarded. This latter criterion has been designed to remove the edges resulting from the Purkinje image, since they tend to

12

produce edges that were tightly clustered. Once the reflections were removed, it would be followed by an iterative process that approximates the pupil circumference, refines it and determines the exact pupil boundary. Then the central vertical column of pixels would be determined which was one pixel wide, traversing through the center of the pupil reaching the upper and lower margins of the pupil at its widest extent. The intensity gradient along this vertical meridian would be then determined for each frame and the slope of this gradient was given out as "*Refraction*" for each frame. The diameter of the circle fit was given out as the "*Pupil diameter*" and average pixel intensity across the vertical meridian was given out as "*Fundus brightness*" (Suryakumar et al., 2009).

The algorithm was never tested or used (calibration and validation) on human subjects. The first task was therefore to develop both instrument and the software for a safe use on the human subjects and investigate its validity to measure the dynamic characteristics of accommodation.

1.4   Setting up

The dynamic photorefractor explained previously was connected to the video capture software using a fire wire. Commercially available video-imaging software (Streampix, Norpix Inc., Canada) was used for video-imaging. It works at a sampling frequency of 70Hz with a resolution of 310*200 pixels for monocular measures. The AVI files recorded were then exported to the DPRS for offline analysis to get refractive or accommodative measures. Both the Streampix and the DPRS were installed on an upgraded system for better performance.

The subsequent chapters will talk about the calibration and validation of the DPRS and all the modifications done in the system during the same.

Chapter 2. Calibration of the Dynamic Photorefraction System (DPRS)

2.1 Modifications

Prior to initiating the calibration, adjustment to dynamic photorefraction system (DPRS) proved necessary since the initial human trials of calibration did not yield good success. The algorithm was facing few issues at the level of pupil detection.

2.1.1 Pupil detection issues

The pupil detection capacity of the DPRS was examined. It was found that in case of subjects with darker iris and conditions with reduced retinal illumination due to the use of IR filters/ semi-silvered mirrors (needed in the calibration and experimental design), the pupil fitting algorithm didn't work properly fitting either inaccurate or no pupils. Also, multiple eccentricities were incorporated to increase the working range of the instrument. Human trials of inducing defocus using a proximity change and trial lenses showed that the algorithm was unable to fit a pupil for a defocus value above ±3D. Occasionally, the tear film reflections and the Purkinge image were considered as edge points due to which incorrect pupils and unreliable defocus values were estimated. Pupil size of the subject given out by the DPRS was usually over-estimated by 3-4mm compared to the manual measurements.

These issues had an impact on the inclusion criterion, working range of the instrument, reliability of the gradient profile estimation and the calibration.

2.1.2 Trouble shooting

Once the DPRS was initiated by importing the video, the first step of the algorithm was to identify the pupil margin by detecting all the points that show a sudden shift in the pixel intensity compared to the neighbour pixels. In case of subjects with darker iris and low intensity conditions (IR filters/ semi-silvered mirrors in the optical path), the amount of light reflected back from the eye that reaches the camera was reduced. Furthermore, the intensity difference expected at the level of the pupil border was reduced due to which the algorithm did not work or fit a pupil. Two modifications were employed to address this issue,

First, the software of the DPRS was designed so that the edge of the pupil margin was determined by sampling until the system found neighbouring points that show a strong gradient shift. If the intensity difference between the two nearest neighbours (pixels) was above a pre-determined threshold value set in the algorithm, they were considered as edge points. If any point doesn't cross that pre-set threshold value, the algorithm restarts the search until it got edge points that fit the criterion. In case of subjects with darker iris and/ or under low intensity conditions, the luminance within the pupil was low because of the decreased amount of reflected light from the eye due to which the intensity difference at the level of edge points was less than the pre-determined threshold limit. Therefore, we had reduced the edge threshold values set in the algorithm to make it work in case of low intensity conditions. Second, we had modestly increased the current supply to the IR LEDs to increase the amount of light reflected back from the retina. The American Conference of Governmental Industrial Hygienists (ACGIH) had suggested exposure limits for infrared radiation from both coherent and incoherent optical sources (ACGIH, 2013). These values were based on the current scientific knowledge and with intent to prevent thermal injury of the retina, cornea and the

crystalline lens of the eye. The calculations of corneal irradiance ($0.249mW/cm^2$) and total effective radiance ($0.391W/cm^2$ sr.) at the level of retina were well within the recommended values by ACGIH (2013) for exposure durations greater than 15 minutes. Furthermore, the algorithm was made robust by including the option of selective analysis where a particular profile line or an area of interest could be selected for analysis. The selection of an area of interest reduced the impact of distracting reflections from the tear film, face or even a trial lens which were sometimes unavoidable.
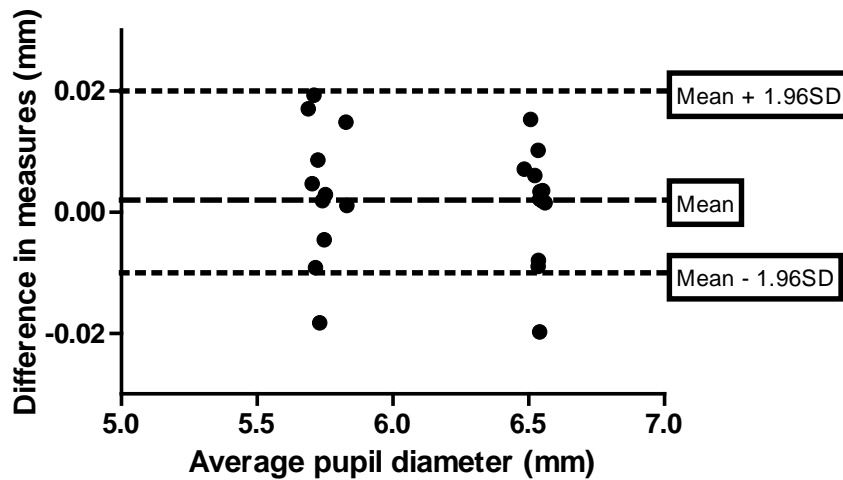
Figure 2-1: Bland-Altman plot showing the agreement between the two procedures used to calculate the pupil size (see text below).

The difference in the pupil measures obtained using both methods were plotted over the average pupil diameter. The mean difference of pupil size measurement (bias) between the two methods was 0.02mm and clinically insignificant. Further, the dispersion of the measures lied within the 95% confidence interval.

2.1.2.1 Accuracy of pupil size estimation

Over estimation of the pupil diameter was found to be due to an improper pixel to millimeter (mm) calibration function originally used in the DPRS. To obtain an accurate calibration factor, an image of a millimeter scale using the photorefractor was taken through which the

number of pixels per millimetre was calculated. The new calibration factor obtained was 11

pixels/mm and was imported into the software.
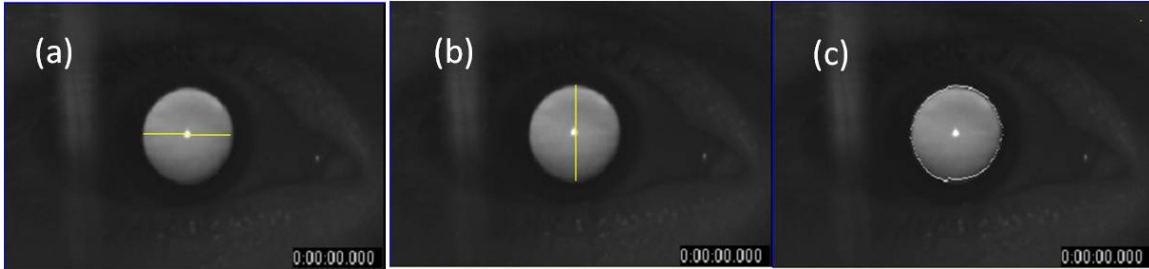
Figure 2-2: Validation of pupil size measurements.

(a) and (b) manual measurement of the pupil size. The height and position of the yellow in the manual component of the algorithm could be changed and allowed us to measure the no. of pixels covered by that line. This pixel value was later converted in to units of mm using the calibration factor and gave a manual measure of the horizontal and vertical pupil size which was averaged later. (c) The pupil fit (white solid circle) by the algorithm measured at the level of each frame.

To assess the validity of the calibration factor, the pupil size in the video files of two subjects

measured by the DPRS was compared to a manual measurement of pupil size. The manual

measurements were measured in pixel units using the profile line method in the manual

component of the algorithm. The pixel units were later converted into millimetre using the

spatial calibration function. 10 frames were randomly selected in a monocular video file

showing a dynamic accommodative response when target proximity (1.5D) was changed.

Bland –Altman plots were used to test the agreement between the two methods. The

maximum deviation between the two methods was 0.02mm which is not clinically significant

(Figure 2-1).

2.2   Why do we need to calibrate?

The output of the defocus measures using eccentric photorefraction is in terms of the

steepness of the intensity profile across the pupil. These intensity patterns need to be

converted into meaningful measures of defocus i.e. into units of diopters (D). Studies (Bobier et al., 1985; Schaeffel et al., 1993) showed that accurate measures of refractive error and accommodation can be obtained only when the photorefractive output is interpreted in terms of calibration obtained from the eye with known refractive defocus. Consequently, a calibration procedure was applied later (Schaeffel et al., 1993) for relative changes in the slope of intensity distribution across the pupil when known refractive defocus was induced. A typical calibration trial involves calculating slopes of the intensity distribution across the pupil when known magnitude of defocus (Both hyperopia and myopia) is induced using trial lens before an eye where the visible light is filtered out using an infra-red (IR) filter. The photorefraction output is regressed on to the values of induced refractive error (accommodative change). As suggested by optical theory the relationship is linear over a finite working range outside the dead zone. The linear equation then defines the relationship between the slope of the intensity profile and the refractive error (accommodation). The slope of the relationship has been termed the conversion factor (Schaeffel et al., 1993).

The conversion factor for a particular individual is normally repeatable i.e. has a low intra-subject variability, but shows a high inter-subject variability (Schaeffel, 1993). This is one of the significant limitations of photorefraction (Howland, 1985; Schaeffel, 1993). The cause is not clear and could arise due to differing retinal reflectance between subjects as well as varying optical characteristics. Schaeffel et al. (1993) showed empirically that the conversion factors didn't show any relation with the pupil size across their experimental sample. However, they showed that the pupil (fundus) brightness level which varies with pupil size showed a negative linear correlation with the conversion factor and suggested that fundus brightness alone could be used to calculate the conversion factor of the subject. That is to say

18

that the effect of individual variations in conversion factors can be normalized by defining them with respect to overall luminance of a given measure. This has been used to allow a set calibration to serve to measure accommodation and refractive error in infants and various animal species without requiring individual calibrations (Schaeffel et al., 1994; Choi et al., 2000). For our purpose we will use both individual calibrations and fundus brightness measures.

A typical calibration trial using the photorefractor involves two steps (Blade et al., 2007; Schaeffel et al., 1993), relative followed by absolute calibration.

- *Relative calibration*: Changes in the photorefractive output was compared when a series of known changes in ocular focus were induced. This is to check the accuracy of the photorefractor in recording the relative changes in the refractive or the accommodative state.
- *Absolute calibration*: Photorefractor output was compared to dynamic retinoscopy when the person fixated at various distances to check its accuracy in measuring the accommodative error.

Absolute calibration of the instrument was shown as part of the validation study (chapter 3) and the subsequent sections in this chapter talk about relative calibration only.

2.3 Methods

2.3.1 Relative calibration

12 normal subjects (Age: 25 to 40 years) were recruited from the School of Optometry and Vision Sciences, University of Waterloo. Those with history of any ocular abnormalities,

history of using any ocular medications or with any binocular anomalies like strabismus or amblyopia were excluded.

The relative calibration as mentioned before was done to see whether the photorefractor output showed a 1:1 relationship with the refractive status. The calibration procedure followed was similar to that used by Schaeffel et al. (1993), where the subject was made to fixate at a distance target with the left eye, while the right eye was occluded with an IR occluder that filters out visible light (allows only IR rays and blocks visible spectrum). Trial lenses ranging in power from +5D to -5D (in steps of 1D) were placed in front of the covered eye for 2-3 sec while the photorefractor records the image. Luminance profiles obtained in each condition were then plotted against the induced refractive error. The slope value of the linear regression fit to this data was then used to convert luminance output given by the photorefractor into diopters (Figure 2-1Figure 2-2).
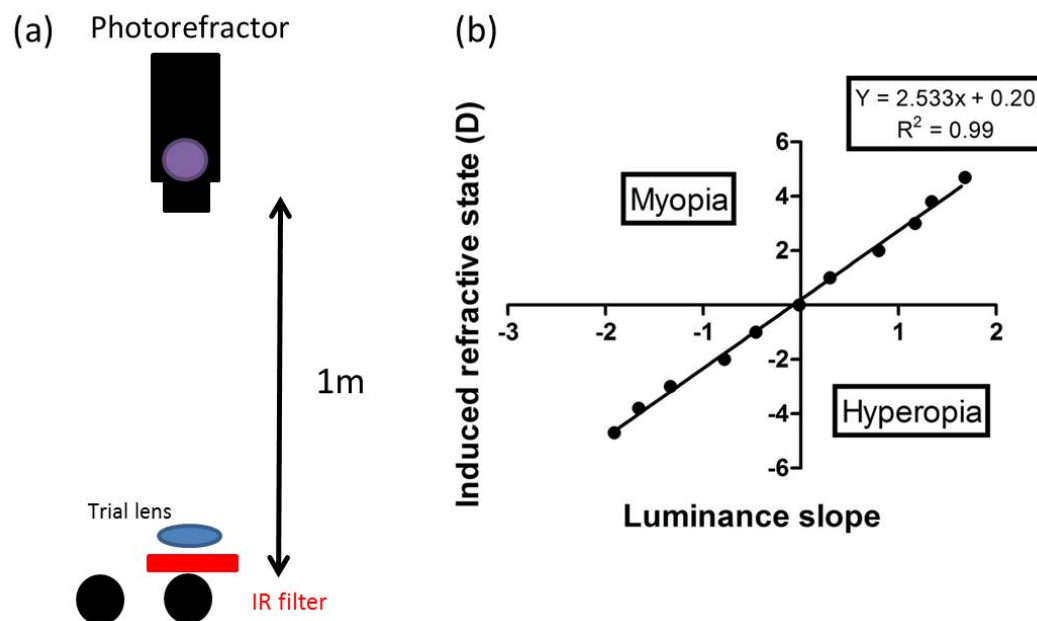
Figure 2-3: Experimental design for calibration.

(a) The photorefractor was aligned with right eye and placed at 1m from the subject. The visible light was filtered out for the right eye using an IR filter while the left eye fixated at a distance target placed on the photorefractor. Lenses ranging from +5D to -5D (in steps of 1D) were placed over the filter for 2-3sec while the photorefractor takes the image. (b) Luminance slope obtained was plotted along the accommodative state (D) induced. The slope of the regression fit was then used as a conversion factor to convert the luminance slope output of the photorefractor into units of diopters.

Repeatability of the measurements was tested on 4 subjects (Age: 25-40 years) by taking the relative calibration measurement of the subject on a different day (within a week from the first visit). Bland-Altman plots were used to test the agreement between the conversion factors obtained during the two visits.

2.3.2   Pupil size calibration

As indicated above, pupil size was to be controlled by considering the luminance within the pupil (fundus brightness). To maintain the accuracy of the response despite a change in the pupil size, an experimental calibration procedure similar to that shown by Schaeffel et al. (1993) was employed. Conversion factor for each subject was plotted over the respective average fundal brightness value obtained from the photorefractor (chapter 1). The slope equation of the linear regression fit was later used to calculate the conversion factor based on the fundal brightness value obtained.

2.4   Results

2.4.1   Relative calibration

The slope of the intensity profile across the refractive state (conversion factor) was calculated on 12 subjects (29.16 ± 3.13 years) and it varied from 1.77 to 3.41 with a mean (± SD) value of 2.86 (± 0.46). Individual calibration slopes along with the average pupil size (mm) and fundus brightness (average grey pixel value across the pupil) were obtained (Table 2-1).

Table 2-1: DPRS output from the 12 subjects along with the repeatability measures.

Subject	Conversion factor	Pupil size (mm)	Fundus brightness (grey pixel value)
First trial			
AM	3.47	7.31	71.38
AN	1.77	7.31	114.45
DT	2.88	7.44	84.13
HW	2.77	8.04	96.45
MV	3.26	7.89	97.54
TB	3.41	7.73	85.67
BA	2.86	7.09	78.18
AH	2.77	7.32	82.66
VC	2.69	7.65	99.81
AlM	2.44	7.65	98.89
CM	3.24	6.72	66.2
KV	2.77	7.58	86.47
Repeatability trials			
TB 2	3.33	7.76	83.39
MV 2	3.2	7.7	95.01
HW 2	2.68	8.05	101.96
DT 2	2.7	6.84	84.02

2.4.2 Repeatability

Conversion factors were obtained on four subjects (30.75 ± 4.11 years) during the repeatability trials on a different day (Table 2-1). A Bland-Altman plot was used to test the repeatability where the difference in the conversion factors obtained in the both the visits was plotted against the average conversion factor between the two visits. As shown in Figure 2-4, all the points were within the 95% confidence intervals (mean ± 2SD) and the coefficient of repeatability (COR = mean+2SD) was 0.20 (≈ 0.05D) and was clinically insignificant.
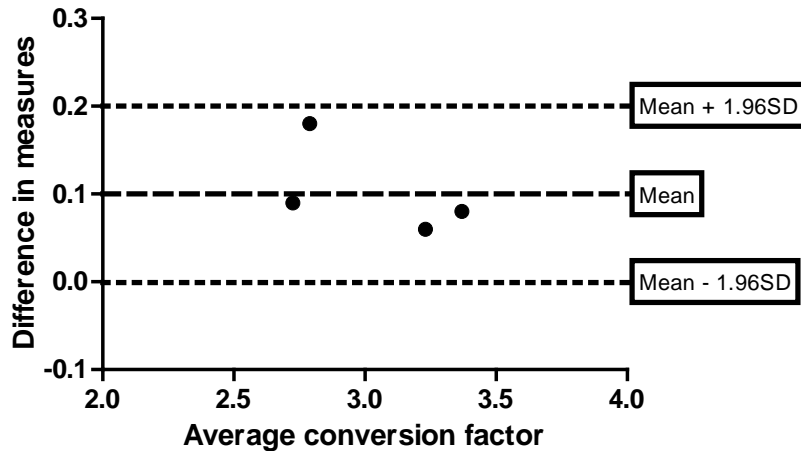
Figure 2-4: Bland-Altman plot suggesting the repeatability of the photorefraction to measure the conversion factor.

The difference in the conversion factors obtained between the two visits was plotted over the average conversion factor. The mean difference in the calculated conversion factor (bias) between the two visits was 0.10. Further, the dispersion of the measures lied within the 95% confidence interval with a coefficient of repeatability of 0.20 which is approximately 0.05D and clinically insignificant.

2.4.3 Pupil size calibration
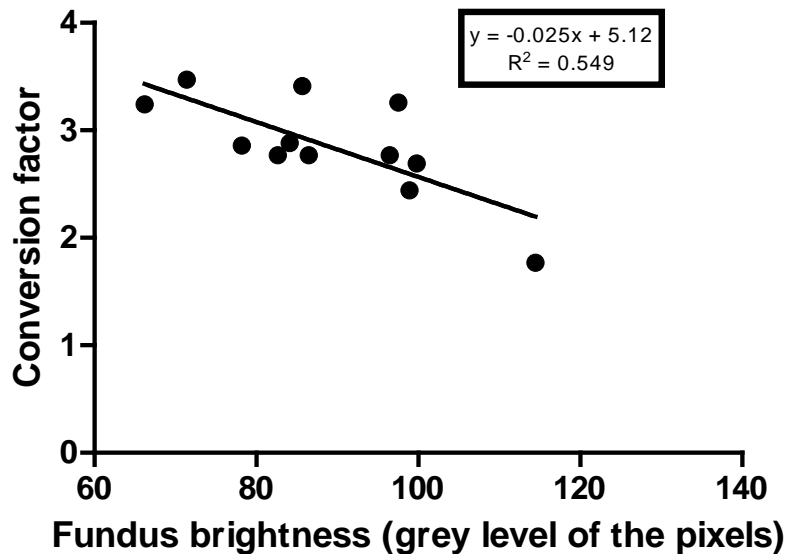
Figure 2-5: Pupil size calibration.

The conversion factors obtained from each subject using relative calibration were plotted against their respective average fundus brightness value. Specifically, as the pupil brightness increased the conversion factor decreased. A linear regression fit to the conversion factor onto the pupil brightness led to the equation y= -0.025x+5.12, where x represents the average fundal brightness value obtained from the subject at that particular frame and y is the conversion factor to be calculated for that frame.

The conversion factor showed inter-individual variability and in order to determine the parameter that caused this variability, correlations were obtained for conversion factors with the other two output parameters that we get from the photorefraction (pupil size and fundus brightness). Surprisingly the pupil size showed no correlation with a change in the conversion factor (y = -0.03x + 3.13; R^2 = 0.008), while the fundus brightness showed an expected negative correlation with the conversion factor (y = -0.025x + 5.12; R^2 = 0.549). The fundus brightness or the luminance across the pupil is known to be affected by the pupil size and fundal reflectance properties (Schaeffel et al, 1993 and 1994). As shown in Figure 2-4, conversion values varied with the luminance of the pupil.

Roorda et al., (1997) predicted that errors of over a diopter can occur in the refractive estimation when calibration trials done at a particular pupil size were used for a trial involving a larger pupil size (See Figure 1-2). Since accommodation responses involve a change in the pupil size and relative calibration does not account for changes in the pupil size, another calibration procedure was needed to avoid errors in the estimation. As it was difficult to calibrate each individual at a constant and known pupil sizes (For e.g. use of artificial pupils do not replicate an actual change in the pupil size), a different parameter was needed that would be influenced by the pupil size. As shown by Schaeffel et al. (1993), correcting the conversion factor according to the luminance value across the pupil would enhance the accuracy even with a changing pupil size. Hence, this procedure of estimating the conversion factor based on the fundus brightness would be appropriate and was showed to provide accurate estimations (Schaeffel et al., 1993) previously even with larger changes in pupil sizes.

The equation was put into the system to calculate the conversion factor based on the fundus brightness and this was later added to the average bias value obtained for the sample during the relative calibration (Y- intercept value in the slope equation) to enhance the accuracy of the estimation.

2.5   Conclusion

A calibration procedure appears to be complete that is one that can define the dioptric estimate of accommodation from the slope output of the photorefractor over a range of pupil sizes. As seen previously (Schaeffel et al., 1993), an inter-individual variability in the conversion factor was noted with a good repeatability between the visits (Figure 2-4). Further, it was shown that

the use of fundus brightness to calculate the conversion factor is valid and can be used to address the inter-individual variability and also the variation in the pupil size. The equation of $y = -0.025x + 5.12$ can be used to estimate the conversion factor (y) based on the value of the fundal brightness (x). While the use of a luminance corrected conversion factor allows a universal calibration (Schaeffel et al., 1993) for all individuals, more accurate results could be obtained by doing individual calibration for an individual bias value (photorefraction error) along with the use of the above equation to adjust for luminance changes resulting from pupil size changes during accommodation. Otherwise errors could be introduced when pupil constriction arises during higher levels of accommodation that could lead to the underestimation of the accommodative response. At the end of the calibration study we had two equations to convert the slope output in to units of diopters. First being the relative calibration where y (diopters) = (Individual calibration slope) (luminance slope output) + (individual bias) and the second being pupil size calibration where y (diopters) = (fundus brightness based conversion factor) (luminance slope output) + (average bias).

Modifications made during the process made the DPRS more robust with a good working range (linearity noted from +5D to -5D without any saturation), and accurate pupil size estimation. Also, modifications involving selective analysis in the DPRS where a profile line or area of interest can be selected helped in reducing the impact of unavoidable tear film and other reflections. The next chapter will be focused on validating the dynamic photorefraction system to measure the dynamics of an accommodative response.

Chapter 3 Validation of the Dynamic photorefraction system (DPRS)

3.1 Purpose and rationale

The purpose of this study was to validate the new dynamic photorefraction system (DPRS). As introduced in the earlier chapter, this instrument was designed to measure the dynamics of accommodative response in younger age groups. Accordingly, the main objective of the study was to see if the newly designed instrument had the ability to accurately measure the dynamics of the accommodative response. Accommodation can be stimulated using blur, retinal disparity or proximity (described in detail in the subsequent sections) but for the purpose of validation, we have limited the measures to only blur-driven accommodation.

3.2 Introduction

Validation is done in order to show that the new instrument (or product) meets the expected standards similar to the existing instruments (or product) based on a similar principle and is able to perform the required procedures without any problem. Photorefraction has been widely used as a screening tool primarily in young children to identify amblyogenic factors of high refractive error, anisometropia and in some cases strabismus (Choi et al., 2000). Additionally, commercial products such as the Power Refractor (Multichannel Systems, Germany) have provided research group the opportunity to obtain dynamic measures of accommodation, refractive and some alignment measures of vergence, typically in infants and children (Schaeffel et al., 1993; Blade et al., 2006). However these capacities were best exemplified in the Power Refractor which is no longer supported, and runs on outdated operating system (Windows 98). Further, the dynamic measures are limited by its resolution of only 25Hz. New fire wire cameras now provide higher resolution (Suryakumar, 2005). Since we are interested

in measuring the dynamics of ocular accommodation in children with myopia, the main objective of the study was to validate the instrument to see if it can accurately measure the dynamics of ocular accommodative response.

3.2.1   What is accommodation?

Accommodation is a dynamic change in the optical (dioptric) power of the eye, allowing the point of focus of the eye to change from a distant to near object (Glasser, 2011). This change in the dioptric power is achieved by changing the curvature of the crystalline lens (anterior > posterior) with the help of lens capsule, zonular fibers and the ciliary muscle (accommodative apparatus). The most widely accepted theory of accommodation was first given by Helmholtz (Hartridge, 1925), later modified by Fincham (1937). According to this theory, in an unaccommodated state (or relaxed state), the ciliary muscle fibers relax, which in turn causes an increased tension in the zonular fibers. This tension draws the lens to a less spherical (flatter) shape which reduces its dioptric power. With a stimulus to accommodation, the ciliary muscle contracts and releases the tension over the zonular fibers. This allows the elastic forces of the lens capsule to mold crystalline lens into a spheroidal shape, thus increasing the dioptric power of the eye. Furthermore, there is a decrease in the equatorial diameter of the crystalline lens, increase in lens axial thickness, and a change in the curvature of the lens (anterior > posterior) resulting in an increase in the refractive power. Retinal blur is considered as the primary stimulus for the accommodation system (Fincham et al., 1951; Heath, 1956; Phillips et al., 1977). Further, accommodation can be stimulated both by the retinal disparity (Heath, 1956; Fincham et al, 1957; Kent, 1958) and by changing the apparent depth (proximity) of the target (Hokoda et al., 1983; McLin et al., 1988; Rosenfield et al., 1990). Accommodation and vergence are seen as cross linked responses, where a change in

accommodation leads to a change in vergence and a change in vergence leads to a cross coupled change in accommodation (Heath, 1956; Fincham et al., 1957).

3.2.1.1 Static aspects of accommodation

Accommodation is expressed in terms of diopters (D). The stimulus to accommodation (AS) is most easily defined in diopters where a D is the reciprocal of the target distance in meters. The accommodative response (AR) refers to change in the optical power of the crystalline lens and this value in D is reciprocal of the metric distance to a plane conjugate with the retina. In an ideal optical system, the accommodative response exerted is equal to the stimulus. Contrarily, an inappropriate response would lead to focusing errors. If the accommodative response is less than stimulus demand (AR<AS), then it is called lag of accommodation. Conversely, it is called lead of accommodation if the response is more than the stimulus (AR>AS). The static characteristics of accommodation are well explained using the stimulus/ response curve (Morgan 1968; Ciuffreda et al., 1983). Accommodation is stimulated either by changing the proximity of target or by inducing minus lenses. The slope of the AS-AR curve is typically less than unity (Morgan et al., 1968) and is attributed to the change in the pupil size that results in an increase in the depth of focus (Ward et al., 1985). Depth of focus is the dioptric range of the focusing error which does not cause a deterioration of the retinal image quality (Atchison et al., 1997)
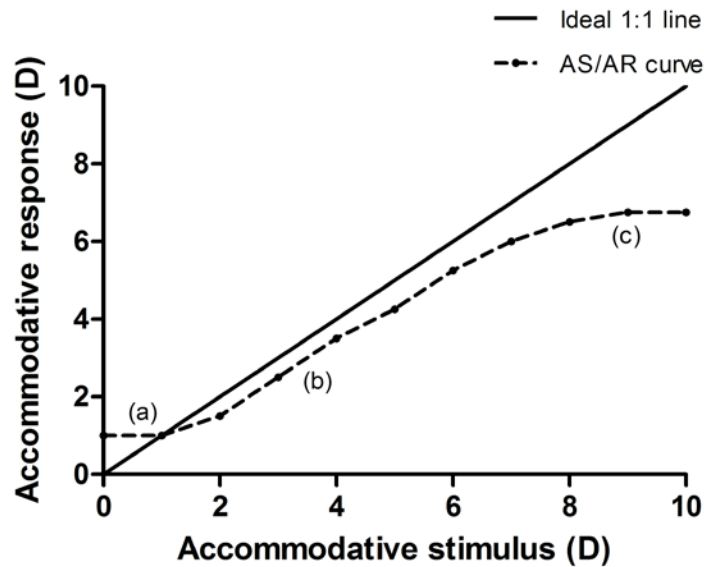
Figure 3-1: Accommodative stimulus-response function

The accommodative response (AR) plotted as a function of the stimulus (AS) (adapted from Ciuffreda, 1983). It is typically a sigmoid shaped function. The solid linear line indicates a perfect 1:1 agreement between the accommodative stimulus and response (AS=AR). A typical static response curve can be divided into three distinct zones, (a) the initial non-linear zone (between 0 to 1.0D) where the response is more than the accommodative stimulus (AR>AS). This is attributed to the resting level of the accommodation. (b) Linear zone, where a proportionate increase in the accommodative response is seen with the stimulus. Usually subjects show some lag in accommodation (i.e. AR<AS) in this stage due to the presence of depth of focus (Ogle, 1958; Ward, 1985). (c) Saturation zone or Functional presbyopia, defines the maximum amplitude of accommodation.

3.2.1.2 Dynamic aspects of accommodation

Another way to describe accommodative response is to understand the response characteristics over time (a dynamic response). Several parameters of accommodation can be studied over time like the latency, response time, amplitude, peak velocity, time taken to peak velocity and acceleration (Figure 3-2).
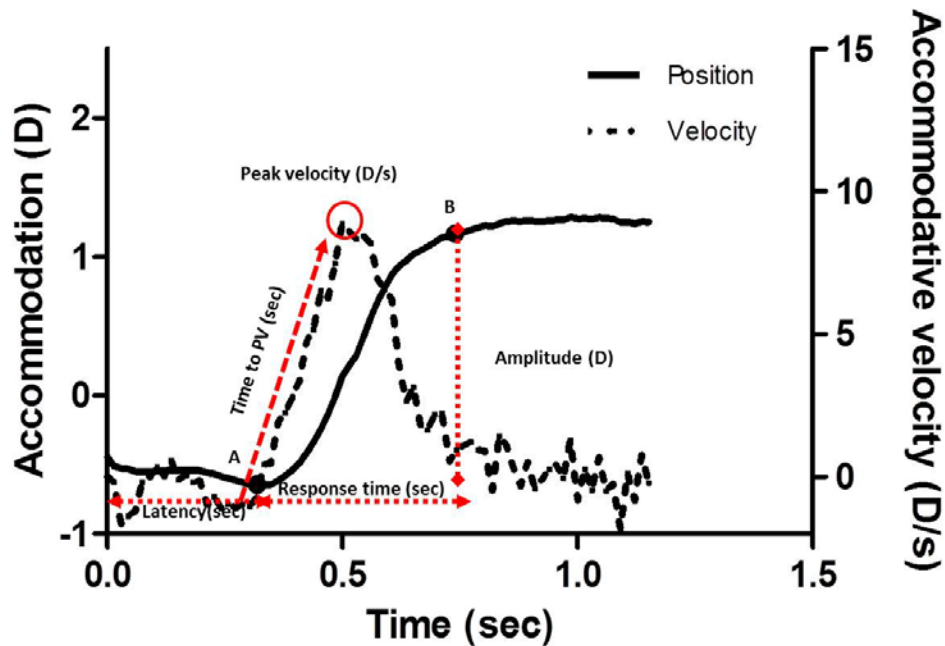
Figure 3-2: Dynamics of an accommodative response.

A typical accommodative response with a lag (solid line) shown for a 2D step stimulus which occurred at 0 sec. Latency (sec) is the time taken to initiate an accommodative response after the start of a stimulus at 0 sec. The dioptric difference between the start (A) and the end point (B) of a response is called as amplitude of the response (D). The time between the start and the end points of a response is called as the response time or the movement time. Differentiation of the response trace over time results in the velocity trace. Peak velocity (D/sec) is the maximum velocity attained during the response (Dotted trace) while the time taken to reach that point from 0D/sec is called time to peak velocity.

Other characteristic dynamic parameter used in various accommodation studies (Ciuffreda et al., 1988; Kasthurirangan et al., 2003, Bharadwaj et al., 2005; Suryakumar et al., 2005) is the main sequence. It is the peak velocity of the accommodative response plotted over the amplitude of the response. The main sequence plot shows how the dynamic mechanism of the accommodation system responds with increasing stimulus demand. Also the mechanism underlying the duration of the eye movement can be calibrated. Main sequences of eye movements were first used to describe the saccadic eye movement mechanism (Bahill et al., 1975) and were later applied to the accommodative system (Ciuffreda et al., 1988). Following that, various studies (Kasthurirangan et al., 2003; Mordi et al., 2004; Bharadwaj et al., 2005;

31

Suryakumar, 2005) showed main sequence over a range of stimulus amplitude. Linearity of the main sequence between the peak velocity and stimulus amplitude was seen over a smaller range of stimulus amplitudes (Ciuffreda et al., 1988; Bharadwaj et al., 2005; Suryakumar et al., 2005) but disappeared with larger range of amplitudes (Kasthurirangan et al., 2003). Recently, second order dynamics of the accommodative response like acceleration, total duration of acceleration and its main sequence were studied (Bharadwaj et al., 2005; Suryakumar et al., 2005; Schor et al., 2006; Maxwell et al 2010). The idea of measuring higher order dynamics was first shown to better understand the vergence responses (Alvarez et al., 1999) and was later studied in an accommodative response (Bharadwaj et al., 2005).

The dynamic characteristics of each component of accommodation, blur-driven accommodation (Campbell et al., 1960; Kasthurirangan et al., 2003; Mordi et al., 2004; Bharadwaj et al., 2005; Suryakumar et al., 2005), convergence accommodation (Suryakumar et al., 2005) and proximal accommodation (Ciuffreda et al., 1988) were examined. These studies (Ciuffreda et al., 1988; Suryakumar et al., 2007) showed that the dynamic characteristics of accommodation like the latency, peak velocity, response time etc. do not differ based on the component (blur/ vergence/ proximity) that stimulated the response.

3.2.1.2.1 *Dynamics of blur driven accommodation*

The first study to look at the dynamics of accommodation using an infra-red optometer was by Campbell et al. (1960). They showed that the average accommodative latency was about 360 msec with a maximum velocity of about 10D/s for 2D step stimulus. Later, various studies (Stark et al., 1965; Phillips et al., 1972; Shirachi et al., 1978) showed that the accommodative latency varied from 300-500msec with a total response duration of about a second (Sun et al., 1986; Heron et al., 1989; Suryakumar, 2005). The main sequence of accommodation has been

studied extensively over a wide range of accommodative demand with a few who showed a linear relation of the peak velocity with the stimulus amplitude (Ciuffreda et al., 1988; Mordi et al., 2004; Bharadwaj et al., 2005; Suryakumar et al., 2005) over a range of smaller accommodative amplitudes which disappeared when a larger range was selected (Kasthurirangan et al., 2003). Further, recent studies (Bharadwaj, 2005; Suryakumar, 2005) on the first and second order dynamics of blur driven accommodation have suggested that peak velocity increases with the stimulus amplitude while the peak acceleration remains constant. Also, the response dynamics were shown to vary with the starting point of accommodation (Suryakumar, 2005; Kasthurirangan et al., 2006).

3.3   Modifications

Early validation trials showed high leads of accommodation response which did not agree with the results of the dynamic retinoscopy (gold standard) thus proving to be unsuccessful. Several modifications were made in the experimental design in order that the problem leading to the inaccuracies in the accommodative response was fixed. The modifications in the design were broadly divided into two types, stimulus related and algorithm related modifications.

3.3.1   Stimulus related modifications

The *targets* used to stimulate accommodation were two high contrast vertical lines. We thought that in order to keep the lines always clear and sharp, subjects were exerting more voluntary accommodation which might had caused a lead in the response. To check the impact of target characteristics on the response, we compared the accommodative response exerted to vertical line target to a letter (ABC) target on 2 subjects. There was no improvement in the estimation of response with a change in the target.

The instrument *dead zone* was the next factor that was considered. Our dead zone calculations on 5 subjects and previous calculations (Suryakumar et al., 2009) on this instrument showed a value of 0.50D. As explained in the first chapter, a dead zone causes uncertainty in the measurement of the refractive error. So we wanted to see the impact of having the far target closer to the subject rather than keeping it at infinity. Also considering the working distance of the photorefractor (1m), we brought the far target to 1.5D and compared it with target being at infinity in a Badal optical system on 3 subjects. The accommodative demand was kept constant (1.5D and 2.0D). There was a marginal improvement (0.1-0.2D) in the accuracy in the estimation of the response but still with a lead in the response.

The *IR filter* used for accommodation trials (Edmund optics, IR transmission ≈ 90%) was different from the filter used for calibration (Hoya, IR transmission ≈ 88%). We expected that this might have caused a difference in the conversion factor measurements. We compared both the filters to calculate the conversion factor on one subject (LH). Conversion factor obtained with Edmund optics filter (3.25) was not different from the one obtained with Hoya filter (3.39) and resulted in a change of about 0.1D in the defocus estimation.

The impact of *alignment* of the eye in relation to the camera was tested in three different ways, eye position (eccentricity), camera position (position) and lens position (tilt).
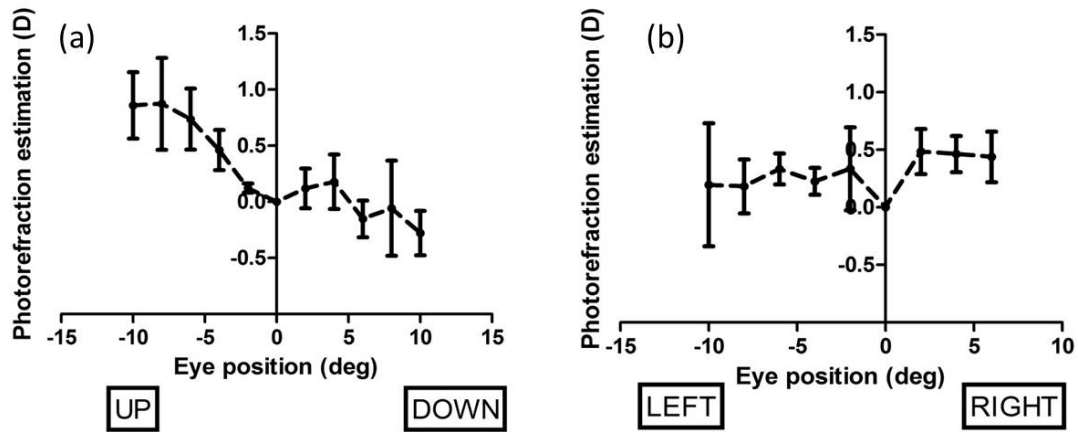
Figure 3-3: Off-axis errors shown by three subjects.

The defocus value in the units of diopters was plotted over the eye position eccentricity. The error bars indicate the standard deviation of the estimation seen between the subjects at that particular eccentricity. There was a consistent change in the defocus estimation in all the gazes. An upper shift in the eye position showed a larger defocus change of about 1.0D compared to other gazes which showed a change of about 0.5D.

A change in the *eye position* (off-axis error) was considered to have had influenced our algorithm. Earlier setup used to stimulate accommodation consisted of targets at different proximities positioned one above the other causing a vertical eye movement with a switch in the stimulus. To investigate the impact of the eye movement on the estimation of defocus, we measured the slopes of the intensity profiles across the pupil when the eye looked at targets placed at various eccentricities (±10 degrees in all gazes) with a constant camera position. Upper shift in the eye position consistently showed an increase in the estimation (Figure 3-3) by approximately a diopter compared to an eye position change in other gazes (estimation change ≈ 0.5D)

35
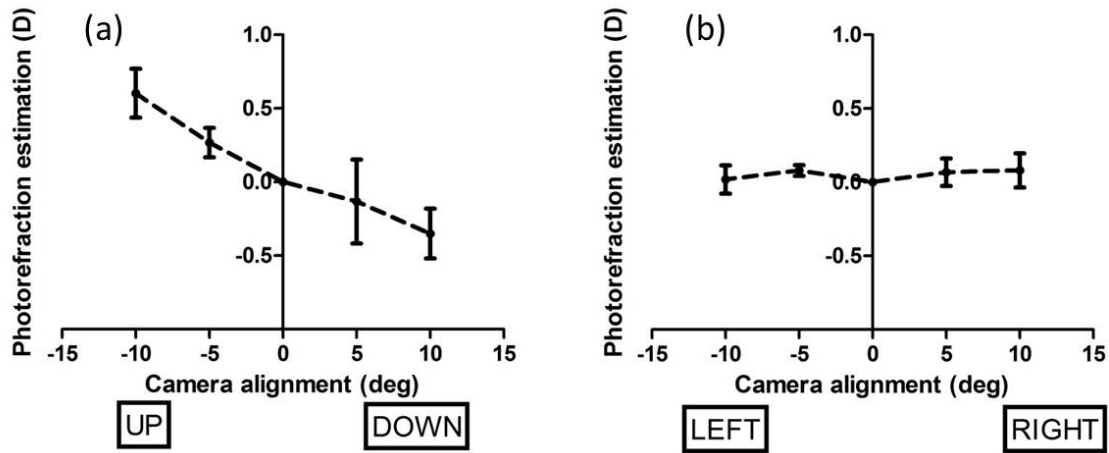
Figure 3-4: Impact of camera misalignment (degrees) on the defocus estimation (D).

The defocus estimation in the units of diopters was plotted over the camera alignment (degrees). The error bars indicate the standard deviation of the estimation seen between the three subjects tested. There was a consistent change in the defocus estimation with a vertical misalignment. A vertical misalignment ($\approx 0.5D$) showed a larger shift in the estimation compared to a horizontal misalignment ($< 0.1D$).

The impact of the *camera position* was tested by tilting the camera up to 10º (5 degree steps) in all the gazes with the eye in a constant position. The camera was moved accordingly to keep the subject's eye in the center of the video image. A vertical misalignment had a much greater impact on the defocus estimation compared to a horizontal misalignment and this could be due to the change in the eccentricity of the source, working distance etc. (Figure 3-5). Our results were consistent with predictions made previously (Bobier et al. (1985); Roorda et al. (1997)) that the slope of intensity profile across the pupil (or height of the crescent) varies depending on the critical optical parameters (discussed in the Chapter 1; Figure 1-3) like eccentricity of the source and working distance.
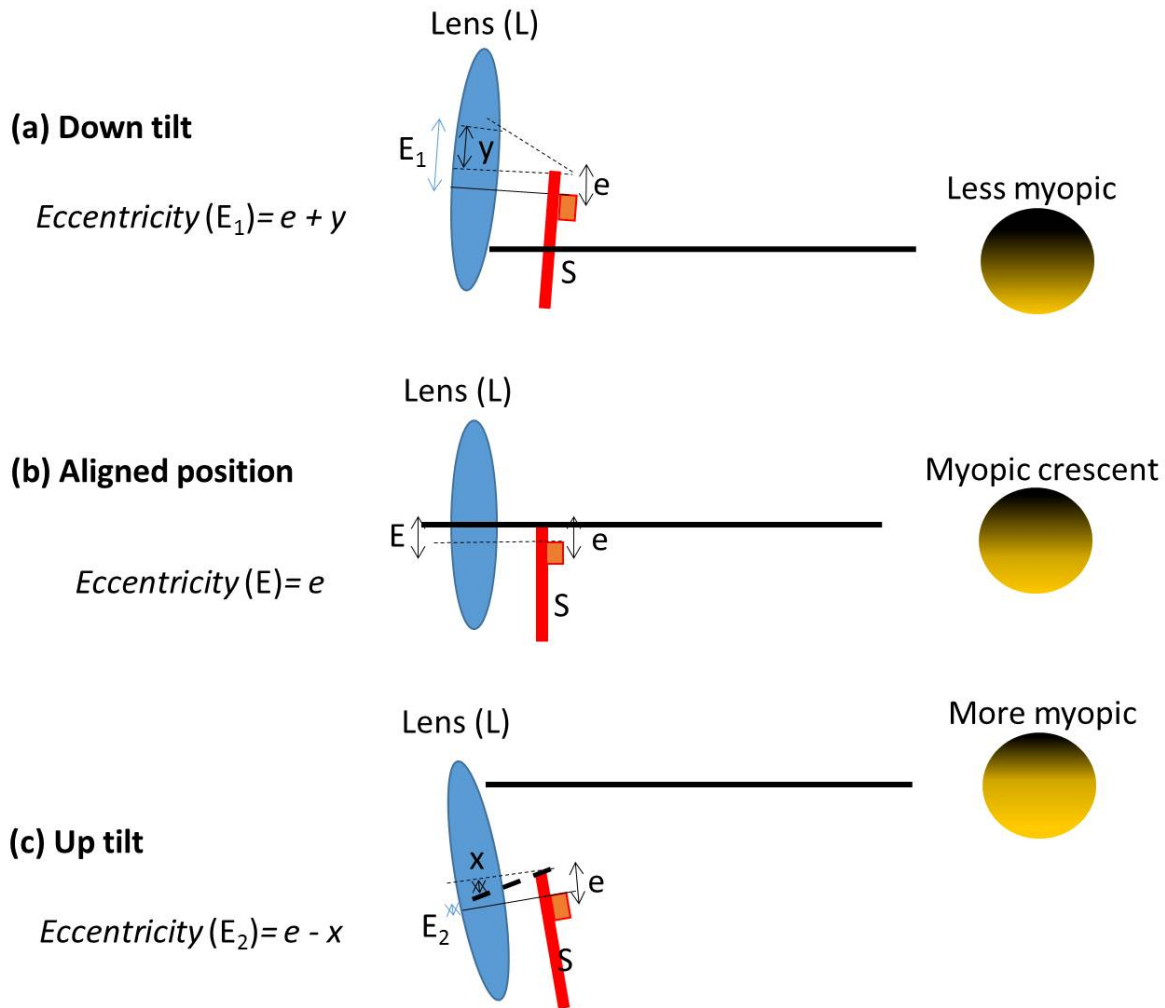
Figure 3-5: Impact of alignment on the critical optical parameters that decide the slope of the intensity distribution across the pupil.

The optical axis of the eye is represented by the black solid line. The actual eccentricity of the source from the camera aperture is defined at the plane of the entrance pupil of the lens L. Since the source (S) sits in front of the entrance pupil, alignment of the eye to camera becomes important. When aligned (b) the extent of eccentricity (e) is similar at the plane of the source and at the plane of the entrance pupil (E). (a) When the source is inferior and the eye is down with respect to the camera, the extent of eccentricity changes. Although the eccentricity at the plane of the source remains unchanged (e), the eccentricity at the plane of the entrance pupil changes by amount y since there is a change in the angle at which the reflected light from the eye enters the camera. Therefore the effective eccentricity at the plane of the entrance pupil on the lens (L) is E_1 (that is e + y). (c) Similarly when the camera is moved down and tilted in the opposite way or when in the eye is up with respect to the camera, the effective eccentricity at the plane of the entrance pupil changes by x, making the effective eccentricity of the source to E_2 (e – x). These changes in the eccentricity automatically change the amount of light reaching the camera thus having an impact on the slope of the intensity across the pupil (as seen in the photorefraction images on the right).These results were in agreement with the theoretical predictions shown by Roorda et al. (1997) using optical ray tracing technique. They predicted that the rate of change on the slope with defocus and the slope value for a particular dioptric defocus increased with a decrease in the eccentricity of the source.

Furthermore, as described before, relative calibration was done using trial lenses placed in-front of the eye and calculating the respective slope value in each condition. The impact of *lens de-centration and tilt* was tested on two subjects using a 2D lens which was moved and tilted in all the four directions (up, down, left and right). The change in the slope value used (conversion factor) for dioptric estimation with a change in the position and tilt of a 2D lens varied from 0.1-0.3 ($\approx$0.1-0.3D) between the subjects and was clinically insignificant.

Also, as indicated previously in chapter 1 and 2, a change in the *pupil size* during accommodation should be accounted to avoid erroneous results in the estimation of the defocus (Figure 1-2). To test the efficacy of the pupil size calibration to account for the change in the pupil size, we compared the accommodative responses with and without 2.5% phenylephrine hydrochloride (PHCl) on 2 subjects. Phenylephrine is an eye drop commonly used in optometry practice to dilate the pupil for fundal examination. There was an improvement in the estimation of the accommodative response by about 0.5 - 1.0D in both the subjects. We came out with two conclusions after examining the videos in this trial. First, the change in the slope of intensity profile across the pupil when eye switched from one distance to other was brought out due to the change in the defocus state of the eye and not merely due to a change in the pupil size. Second, the pupil size calibration failed to account for changes in the pupil size in few subjects during a dynamic accommodation response causing a lead.

3.3.2 Algorithm related modifications

Individual calibration trails included inducing lenses ranging from +5D to -5D. But since our measurements mostly range between 0 to +5D, we have altered the method of calculating the *conversion factor*. Rather than choosing a wide range (+5D to -5D), we decided to use only the plus lens section of calibration to calculate the conversion factor because that covers the

actual data range of our study. Vertex distance compensation was applied to +4 (3.8D) and +5D (4.69) lenses to enhance the accuracy in calculating the conversion factor. Furthermore, the plot between the fundus brightness and conversion factor (pupil size calibration) based on the modified data showed an equation $y = -0.008x + 2.66$; $R^2 = 0.73$. This equation was later used to calculate the conversion factors which further were used to estimate the defocus in units of diopter.

As described earlier in Chapter 1, once the algorithm identifies the pupil and refines the fit, the slope of the intensity profile was calculated from the upper to the lower edge of the pupil. Further, previous study (Suryakumar et al., 2002) at our lab showed that the slope of the intensity didn't statistically vary with the *height of the profile* measured within the pupil. But, we have noted in few of our subjects that due to some unknown reasons the upper half of the pupil is more brighter than the bottom half or vice versa, causing a hyperopic/myopic shift in the defocus estimation. So we wanted to see the impact of reducing the height of profile line in those subjects. A large variability was noted in the slope value with a change in the height of the profile line. The discrepancy with the earlier results could be due to the differing defocus patterns resulted from the lenses (Suryakumar et al., 2002) compared to those resulted due to proximity (the present study). Also both the studies used smaller samples with high variability that might not have represented a larger population. Hence, further work on a larger sample is necessary to understand the impact of profile line width on the estimation of defocus.

3.4 Methods

Seven adult (20-35 years) subjects and two children (10-15 years) were recruited from the Optometry clinic at the School of Optometry and Vision sciences, University of Waterloo.

Subjects who were ametropic were corrected using contact lens during the study. Subjects with any ocular abnormalities or with any history of using ocular medications were excluded. Further, those with any binocular anomalies like strabismus (eye deviation), amblyopia (lazy eye) were excluded. The study received ethics approval from the Office of Research Ethics (ORE), University of Waterloo and all the subjects were provided an informed consent prior to start of the study.

3.4.1 Experimental design

A Badal optical system was used to stimulate the accommodation. The Badal optical system was chosen because the perceived angular distance of the target would be always being constant even after a change in the dioptric demand for accommodation (Atchison, 1995). The targets were two high contrast vertical lines (white on black) illuminated using light emitting diodes (LEDs). A 2D stimulus was provided by placing the distance target at 17cms (0.75D) from the 5D Badal lens and the near target was at 9cms (2.75D) from the lens. A step stimulus was created where only one target was lit at a time. The change in the target position was achieved using a switch controlled by the experimenter. This switch was connected to an input-output control box that was further connected to the video software allowing a time stamp to be created when targets were switched. As seen in figure 3-6, infra-red filter was used in order that the presentation of targets was achieved along with a continuous measure using the dynamic photorefractor. A semi-silvered mirror was used in the Badal optical system to align the targets at two different positions close to a constant axis. This avoided the need for an eye movement with a switch in the target position. All the subjects were instilled with 2.5% phenylephrine hydrochloride (PHCl) in their right eye to keep the pupil size relatively constant.
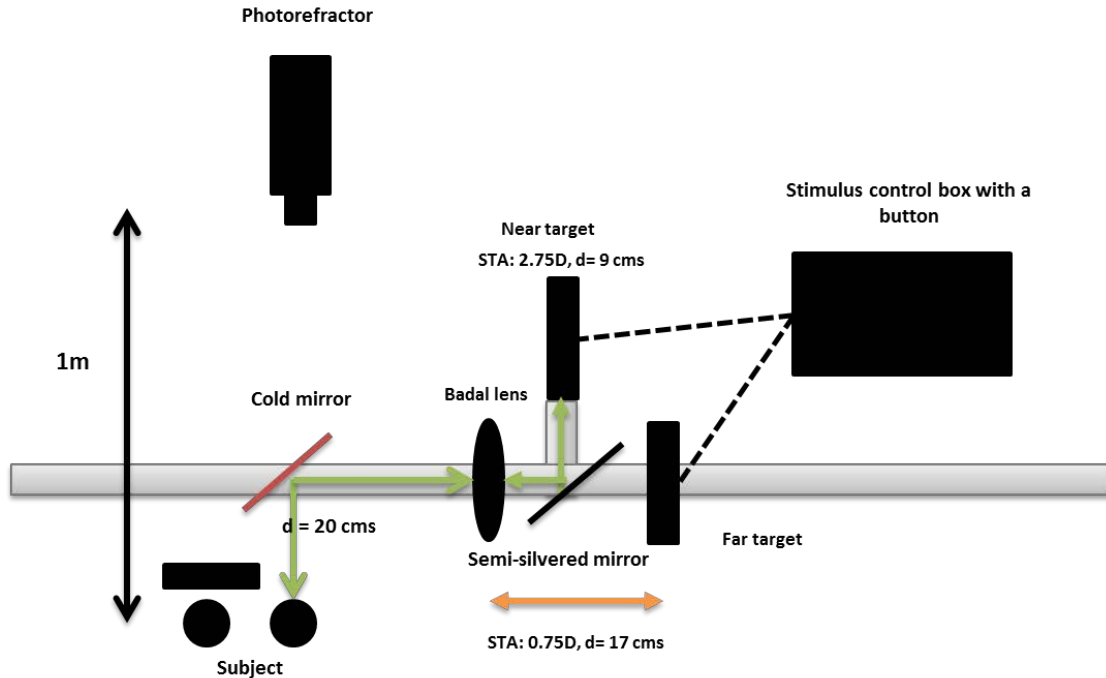
Figure 3-6: The experimental design for stimulating accommodation.

The photorefractor was placed at 1m from the subject. A Badal optical system was used to stimulate accommodation with a constant angular distance. A cold mirror (IR filter) was used in order that target presentation is done along with a continuous measurement using the photorefractor. A semi-silvered was used in the optical path to align the targets one above the other. A 5D Badal lens was used and targets were placed accordingly to stimulate a step change of 2D in accommodation.

3.4.2 Dynamic photorefractor

The dynamic photorefraction system (DPRS) explained in the earlier chapters was used to estimate the accommodative response along with the pupil size. The dynamic photorefractor was connected to the system using a fire-wire. Commercially available video acquisition software (Streampix, Norpix, Canada) was used for recording the images of the eye. The dynamic photorefractor worked at a sampling frequency of 70Hz, giving an output every 0.014 seconds. The photorefractor was placed at 1m from the subject with an IR filter in place to allow target presentation along with a continuous photorefraction. The video images were later analyzed in the offline application described in the first chapter. Slope measures across

the vertical meridian of the pupil were outputted into EXCEL sheet along with the fundus brightness and pupil diameter in each frame.

3.4.3 Procedure

Retinoscopy was done prior to the start of the study and the baseline refractive error was recorded. The right eye of the subject was dilated using 2 drops of 2.5% phenylephrine hydrochloride (PHCl) after an initial anterior chamber assessment of the subject. Phenylephrine was showed to have an impact on the amplitude of the accommodation and the response time of accommodation (Mordi et al., 1986; Sarkar et al., 2012). However, a reduction in the static and dynamic aspects was not expected to influence our purpose of validating the instrument. All the subjects were individually calibrated to obtain a calibration function or conversion factor which was later used to convert the slope output of the subject into units of diopters.

Subjects were given 2-3 practice trials prior to the start of the study to familiarize them to the study procedures and the task of changing their focus with the switch in the stimulus. All the measurements were taken from the right eye of the subject while the left was covered using an occluder or an eye patch. During the experiment, subjects were clearly instructed to keep the edges of the vertical lines clear and sharp at all times. The target was alternately illuminated using the button and onset of the stimulus was randomized to avoid prediction of the near target or the accommodative stimulus. 3-5 accommodative trials were taken for the 2D step stimulus with a 4 sec presentation time. The responses were later analyzed and averaged. Subjects were given a break in between the calibration trial and the accommodation trials. Dynamic retinsocopy was also done on the right eye to measure the lag or lead in the accommodative response for a target at 50cms.

3.4.4   Analysis

3.4.4.1 Dynamics of accommodation

The recorded video file was first loaded into the DPRS for analysis. The DPRS as described previously in chapter 1 would analyze the video file and output the slope of the intensity profile along with the pupil diameter and the fundal brightness at the level of each frame. The slope values obtained were converted into units of diopters using conversion factors obtained from both relative and pupil size calibration (using the equation $y = -0.008x + 2.66$). The raw position data for the step stimulus obtained from the DPRS was later imported into MATLAB where it was plotted over time. A 2 point differentiation technique was used to get the velocity profiles (D/s) which were later smoothened using a 100msec window (Bharadwaj et al., 2005). A MATLAB script (Appendix D) based on the velocity threshold criterion (Schor et al., 1999; Bharadwaj et al., 2005; Suryakumar, 2005) was used for analyzing the start and end point of the response in a position trace. The start of the response was located by looking for a point where the slope exceeded 0.5D/s and continued to do it for another 100 msec (7 frames). The second section of 100 msec continuation window was chosen to avoid false positives. Conversely, when the slope was less than 0.5D/s and continued the same for the next 100 msec, it was identified as the end point of the response. These points were later inspected to check the accuracy. Later, they were used to analyze the dynamic characteristics latency, response time and amplitude of the accommodative response. Latency was defined as the difference in the time value between the onset of stimulus and the start point. Amplitude was the difference in the accommodative position at the start and end point. Response gains were calculated from the amplitude data wherein the gain was defined as the ratio of accommodative response over accommodative stimulus. Response time was the difference in

43

the time value at the start and end points. Peak velocity was the maximum velocity value in the smoothened velocity profile. Time to peak velocity was time taken to reach that peak point from 0D/s of velocity.

3.4.4.2 Accuracy of DPRS

The photorefraction data were analyzed in two different ways for each subject. First, using the conversion factors obtained from individual calibration (using lenses) and second, using the pupil size calibration (As explained in Chapter 2). Bland-Altman plots were used to compare the agreement between the two methods in estimating the response gains. Furthermore, the methods were compared to the gold standard dynamic retinoscopy to check the accuracy.

3.5 Results

Calibration and accommodation trials were performed on 9 subjects (7 adults (29.57 ± 2.69 years) and 2 children (11 ± 1.4 years)). Individual conversion factors were obtained from all the subjects and it ranged from 1.48 to 2.08. Four out of nine subjects (AX, KR, PH, and VJ) showed sluggish accommodative responses with either flat response traces or those that didn't meet the velocity threshold criterion. Table 3-1 shows the conversion factors and accommodation data of the other five subjects who showed good responses.

Table 3-1: Dynamic characteristics of accommodation in 5 subjects

Subject	AlM	HW	MV	GL	CL
Conversion factor	1.58	1.57	2.02	2.08	1.93
Gain (Retinoscopy)	0.75	0.87	0.75	1.12	0.87
Gain (DPRS)	0.69 ± 0.26	0.77 ± 0.06	0.86 ± 0.19	0.98 ± 0.02	0.92 ± 0.17
Latency (ms)	270.3 ± 30.9	404.1 ± 138.1	450.6 ± 135	383.6 ± 22.3	329.6 ± 49.8

Response time (ms)	351.8±102.3	666±74.5	706.8±224.3	546±92.9	651.3±206.9
Peak velocity(PV) (D/s)	5.88±2.16	4.1±0.53	4.28±1.02	7.95±2.19	5.78±1.26
Time to PV (ms)	128.8±37.1	126.5±41.5	112±40.09	111±22.9	145.6±18.5

Figure 3-7 shows a typical accommodative position trace and differentiated velocity trace over time for a 2D stimulus.
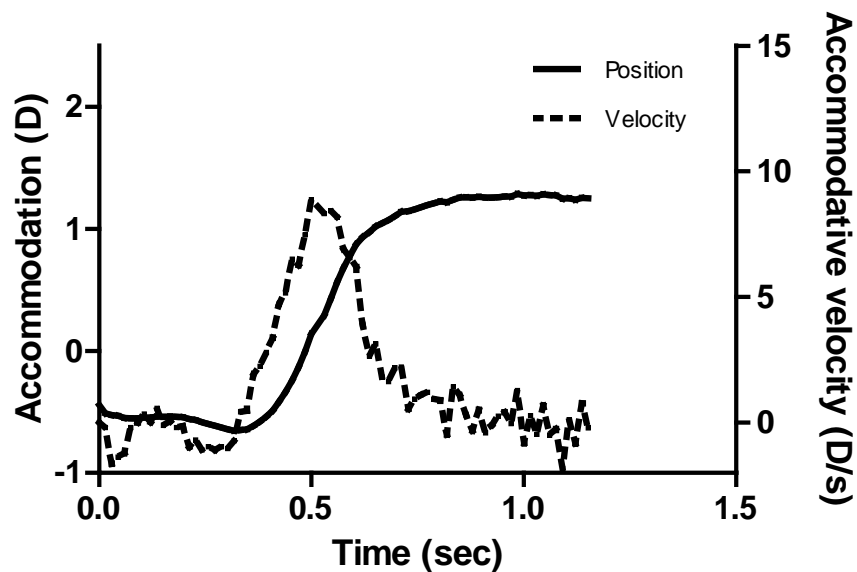
Figure 3-7: Example of a typical accommodative response (solid line) and velocity trace (dotted line) over time for a 2D stimulus.

Accommodation (left Y-axis) and accommodative velocity (right Y-axis) were plotted over time. Both position and velocity traces were smoothened over a 100 msec window. The stimulus was presented at 0 sec and as shown the initiation of the response occurred with a latency of ≈350msec and total duration of the response (latency + response time) was less than a second. A rise in the differentiated velocity profile was noted slightly before the point of response initiation and started to fall as the required accommodative state was achieved. This discrepancy in the initiation of the velocity and position traces was attributed to the smoothing and differentiation procedures followed.

Sluggish accommodative responses were obtained from four subjects with very low gain values (VJ: 0.225; KR: 0.15; AX: 0.17; PH: 0.05). Bland-Altman plots suggest that the gain

values of these four subjects obtained from the dynamic retinoscopy were comparable to the

values obtained from the DPRS (Figure 3-8).
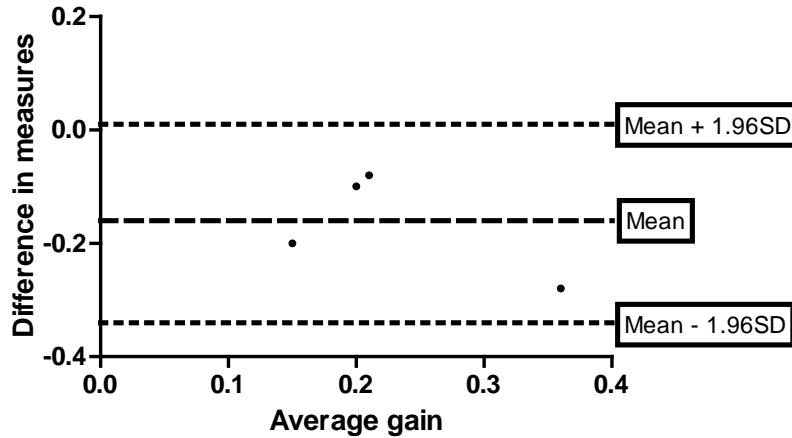
Figure 3-8: Bland-Altman plot showing the agreement between the DPRS (Individual calibration) and the dynamic retinsoscopy in estimating the defocus.

The difference between the gain values obtained using the two methods being compared was plotted over the average gain value of the subject. The mean difference was represented using the heavy dotted line, while the 95% confidence intervals was represented using the light dotted lines. A minus value indicates under-estimation and the contrary indicates over-estimation. The mean difference between the DPRS (using individual calibration) and dynamic retinoscopy was -0.16 (underestimation by 0.3D).

Bland-Altman plots were used to compare the gain values obtained using dynamic

retinoscopy with DPRS using individual calibration, and DPRS using pupil size calibration.

The difference in the gain obtained using the two methods were plotted over the average gain

value. Figure 3-9 (a) shows a mean difference of -0.08 (0.16D underestimation) and

maximum difference of -0.32 (0.64D underestimation) between the retinoscopy and DPRS

(using individual calibration). A slight decrease in the accuracy was noted with DPRS (using

pupil size calibration) with a mean and maximum difference of -0.12 (0.D) and -0.34 (0.68D)

respectively compared to retinoscopy (figure 3-9(b)).

Figure 3-9: Bland-Altman plots showing the agreement between the dynamic retinoscopy and two methods of calculating conversion factors ((a) Individual calibration, (b) Pupil calibration).

The difference between the gain values obtained using the two methods being compared was plotted over the average gain value of the subject. The mean difference was represented using the heavy dotted line and the 95% confidence intervals were represented using the light dotted lines. A minus value indicates under-estimation and the contrary indicates over-estimation. The mean difference between the DPRS (using individual calibration) and retinoscopy (underestimation ≈0.16D) was lesser compared to the DPRS (using pupil calibration) and retinoscopy (underestimation ≈0.24D) and were clinically insignificant.

Furthermore, Bland-Altman plot was used to investigate the agreement between the gains obtained using conversion factors obtained from individual and pupil size calibration. The mean and maximum difference between the two methods (Figure 3-10) was 0.03 (0.06D) and 0.24 (0.48D) respectively.
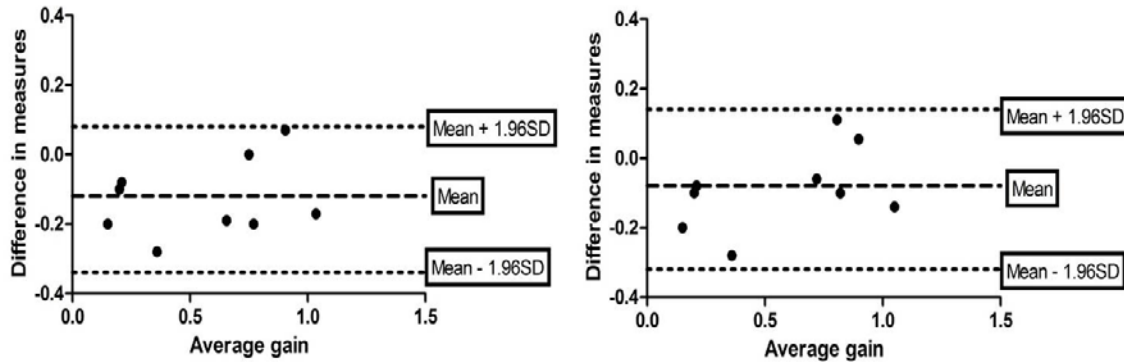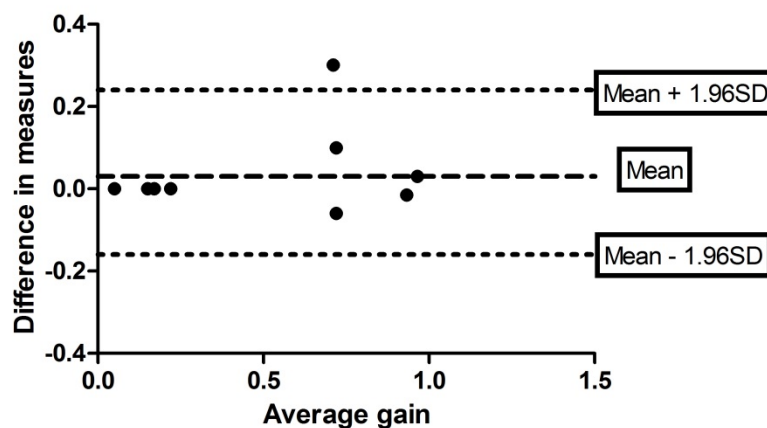

Figure 3-10: Bland-Altman plot showing the agreement between the two methods of calculating conversion factors (Individual calibration and Pupil size calibration).

The difference between the gain values obtained using the two methods being compared was plotted over the average gain value of the subject. The mean difference was represented using the heavy dotted line, while the 95% confidence intervals was represented using the light dotted lines. A minus value indicates under-estimation and the contrary indicates over-estimation. The mean difference between the DPRS (using individual calibration) to the DPRS (using pupil calibration) was 0.06D and was clinically insignificant.

3.6   Conclusion

Dynamic photorefraction system (DPRS) is an offline analysis application used to analyze the video output from the photorefractor. It can acquire quick and accurate estimations of both defocus and pupil diameter provided an individual calibration function is obtained from each subject to enhance accuracy. Unlike the commercially available instruments like Power-refractor, it provides the option of individual calibration, thus enhancing the accuracy of the estimation. Furthermore, it works at a higher sampling frequency that can help us in getting a better picture of the various dynamic characteristics of an accommodative response.

3.6.1   Validation

A number of modifications were done in the process of calibrating and validating this dynamic photorefraction system making it a more robust and dynamic tool to accurately measure the accommodation and pupil size. We had successfully calibrated the instrument and in agreement to Schaeffel et al. (1993) and Roorda et al. (1997), inter-individual variability of the conversion factors was noted due to the differing optical characteristics. As described in the previous chapter, pupil size measures were accurate and in good agreement with the manual measurements (Figure 2-1). Pupil fitting is a very important step in the whole analysis procedure and any error in its fit can lead to erroneous results both in the estimation of pupil size and the defocus. DPRS was designed such that it was able to analyze the brightness profiles conveniently even with pupils as small as 3mm. Accommodative responses were obtained from 9 subjects and the dynamic characteristics of the response were analyzed using

the velocity threshold criterion (Schor et al., 1999; Bharadwaj et al., 2005; Suryakumar, 2005) and the dynamics of the response obtained were in agreement to those shown in the literature (Campbell et al., 1960; Tucker et al., 1979; Suryakumar, 2005). The average (±SD) gain value of our sample was 0.53 (±0.37). The responses for the 2D stimulus were variable with four subjects showing high lags of accommodation and one subject exerting a lead in the accommodative response. Tucker and Charman (1979) showed that the accommodative responses for stimulus up to 2D were usually variable with over shoots and/ or flat responses. They also showed that this response variability can be within and between the subjects. Furthermore, they suggested that the variances in the response could be due to the difference in the depth of focus, resting state of accommodation, and the amount of voluntary accommodation. In agreement with this, the present data showed a high degree of variability in the accommodative gains between the subjects for a 2D stimulus.

Bland –Altman plots showed an agreement between the accommodative gains obtained from the gold standard dynamic retinoscopy and the photorefractor. The difference in the accommodative gains obtained using conversion factors obtained from individual calibration and the pupil size calibration was clinically insignificant (Figure 3-9; Figure 3-10). The average difference in the responses obtained between the DPRS and the dynamic retinoscopy (0.25D) was imported in to the system as a correction factor to enhance the accuracy of the estimation of the refractive state for future studies.

3.6.2 Future work

3.6.2.1 Developments in DPRS

Although the new analysis algorithm had success in measuring the dynamics of accommodation and pupil size measures, the pupil size calibration needs to be more robust to avoid the use of mydriatic drops. The pupil size calibration procedure was done to account for the changes in the pupil size during a dynamic response. Our system did not show a good success rate in fixing this problem in few cases due to which i had to use phenylephrine eye drops to get a relatively constant pupil size for a 2D step stimulus of accommodation. Using ray tracing technique, Roorda et al. (1997) predicted that errors of about a diopter can occur when calibration function calculated at a larger pupil was applied directly to slopes measured with smaller pupils. In agreement with that prediction, our earlier data (prior to the modifications) estimated leads ($\approx$ 1.0D) in accommodation because the pupil size calibration failed to account for the changes in the pupil diameter. A larger sample involving a wide range of pupil sizes would help in establishing a more robust correlation between the conversion factor and fundus brightness (pupil size). Further work would focus on calibrating individuals with smaller pupils and/ or subjects with lower fundus brightness.

3.6.2.2 Experimental design

As the data from this study (Figure 3-3; Figure 3-4) indicated that a vertical misalignment had much larger impact on the defocus estimation compared to the horizontal misalignment, future experimental design will include accommodative stimuli that are displaced horizontally at different proximities that would not account for entrance pupil misalignment more than 10 degree (Figure 3-3; Figure 3-4). This kind of arrangement would allow presentation of accommodative stimuli without causing any significant misalignment errors.

3.6.2.3 Myopia and accommodation

As mentioned in the first chapter, the sole purpose of building this new instrument was to measure the dynamics of accommodation in children with myopia given the limitations of existing photorefraction systems.

Various control theory models were designed to explain the mechanism of oculomotor systems like accommodation and vergence (Hung et al., 1980; Schor, 1992) of which the most widely accepted model was given by Schor (1992). These models were used to describe both static (Hung et al., 1980; Schor, 1992; Hung, 1998) and dynamic (Schor et al., 2004; Schor et al., 2006; Maxwell et al., 2010) aspects of accommodation and vergence. But the findings of high AC/A, high lag of accommodation coupled with high accommodative adaptation in children with myopia doesn't follow the pattern described by control theory models and earlier empirical investigations (Schor et al., 1989). Although tonic vergence (adaptation) appeared to be reduced following the model's prediction (Sreenivasan et al., 2012), preliminary data (Sreenivasan et al., 2014) from our lab suggest that the CA/C measures were normal instead of being reduced. From these results, we hypothesize that high accommodative adaptation could be due to slow accommodative responses and a sluggish accommodative plant (Lens, zonules and ciliary muscle) causing larger response lags with high AC/A. Therefore, in order to prove this hypothesis, the first step is to measure the dynamic characteristics of accommodation in children with myopia. The new user friendly dynamic photorefractor will be used to measure the dynamics of accommodation in children with myopia.

3.6.2.4 Calibration in children

In adults, to enhance the accuracy of the estimation relative calibration equation was used with conversion factor calculated at the level of each frame based on the fundus brightness thus accounting for changes in the pupil size without compromising the accuracy of the estimation. But it is difficult to apply a similar procedure in case of children taking into account their shorter attention spans or limited cooperation. Hence, the tedious relative calibration will be replaced by the pupil size calibration ($Y = -0.008x + 2.66$; where Y is the conversion factor to be calculated and x is the fundal brightness value noted in that particular frame) to calculate the conversion factors and bias (Y intercept) will be based on the average value taken from the relative calibration data of the sample (0.96D). This procedure was shown to have a clinically insignificant impact on the accuracy of the estimation (<0.50D) and is employed as an automated procedure (Universal calibration function) in the commercially available photorefractors (Schaeffel et al., 1993).

Appendix A

Dynamic analysis of accommodation

In order to analyze the dynamic characteristics of the accommodative response, velocity threshold criterion was chosen. Photorefraction data obtained using the high speed photorefractor was converted into an AVI file. The converted video file was then loaded into the DPRS for analysis. The slope of the intensity profile along with the pupil diameter and the fundal brightness in each frame were given out from the DPRS in the form of an EXCEL sheet. The slope values obtained were converted into units of diopters using conversion factors obtained from either individual or pupil size calibration. The raw position data for the step stimulus obtained from this procedure was later imported into MATLAB where it was plotted over time. A 2 point differentiation technique was used to get the velocity profiles (D/s) which were later smoothened using a 100msec window (every 7 frames in our case).
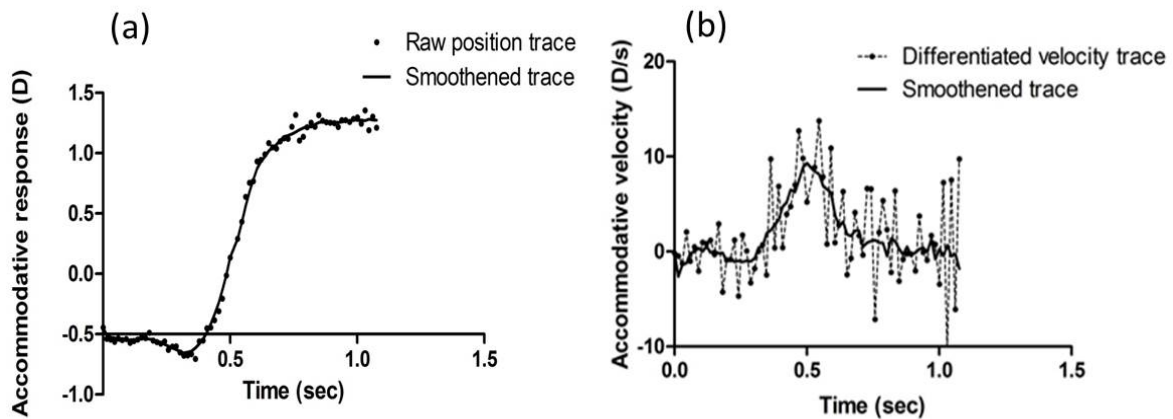
Figure 0-1 Raw and smoothened accommodative position and velocity traces.

(a) Accommodative position plotted over time. Dots represent the raw position data while the solid line represents the smoothened data. Position traces were averaged using a 100 msec (every 7 frames) to smoothen the data. (b) Raw traces of the differentiated velocity profile (dotted line) were smoothened (solid line) using the same 100msec window (7 frames).

The velocity threshold criterion was then applied to the smoothened data to get the start and end points of the response. The start of the response was located by looking for a point where the slope of the velocity profile exceeded 0.5D/s and continued to do it for another 100 msec (7 frames). The second section of 100 msec continuation window was chosen to avoid false positives. Conversely, when the slope becomes less than 0.5D/s and continues to do it for the next 100 msec, it was identified as the end point of the response. These points were later inspected to check the accuracy of the location of the points. Later, they were used to analyze the dynamic characteristics of the accommodative response. Latency was the difference in the time value between the onset of stimulus and the start point of the response. Amplitude was the difference in the accommodative position at the start and end point of the response. Response time was the difference in the time value between the start and end points. Peak velocity was the maximum velocity value in the smoothened velocity profile. Time to peak velocity was time taken to reach that peak point from 0D/s of velocity.

A MATLAB script was generated to automate the procedure of the velocity threshold criterion to analyze the dynamics of accommodation. This script helps in importing, smoothening the data and then apply the velocity threshold criterion over the smoothened data for analyzing the start and end point of the response in a position trace.

Appendix B

Supplier Elsevier Limited, The Boulevard,Langford Lane, Kidlington,Oxford,OX5 1GB,UK

Registered Company Number 1982084

Customer name Vivek Labhishetty

Customer address 529A Waterloo, ON N2L4S9

License number 3438270397759

License date Jul 29, 2014

Licensed content publisher Elsevier

Licensed content publication Computers in Biology and Medicine

Licensed content title Dynamic photorefraction system: An offline application for the

dynamic analysis of ocular focus and pupil size from photorefraction images

Licensed content author Rajaraman Suryakumar, Derek Kwok, Sheldon Fernandez, William

R. Bobier

Licensed content date March 2009

Licensed content volume number 39

Licensed content issue number 3

Number of pages 11

Start Page 195

End Page 205

Type of Use reuse in a thesis/dissertation

Portion figures/tables/illustrations

Number of figures/tables/illustrations 1

Format both print and electronic

Are you the author of this Elsevierarticle? No

Will you be translating? No

Title of your thesis/dissertation: Calibration and validation of the Dynamic Photorefraction

system (DPRS)

Expected completion date Oct 2014

Estimated size (number of pages) 100

Elsevier VAT number GB 494 6272 12

Permissions price 0.00 USD

VAT/Local Sales Tax 0.00 USD / 0.00 GBP

Total 0.00 USD

Terms and Conditions

INTRODUCTION

1. The publisher for this copyrighted material is Elsevier. By clicking "accept" in connection

with completing this licensing transaction, you agree that the following terms and conditions

apply to this transaction (along with the Billing and Payment terms and conditions established

by Copyright Clearance Center, Inc. ("CCC"), at the time that you opened your Rightslink account and that are available at any time at http://myaccount.copyright.com).

GENERAL TERMS

2. Elsevier hereby grants you permission to reproduce the aforementioned material subject to the terms and conditions indicated.

3. Acknowledgement: If any part of the material to be used (for example, figures) has appeared in our publication with credit or acknowledgement to another source, permission must also be sought from that source. If such permission is not obtained then that material may not be included in your publication/copies. Suitable acknowledgement to the source must be made, either as a footnote or in a reference list at the end of your publication, as follows: "Reprinted from Publication title, Vol /edition number, Author(s), Title of article / title of chapter, Pages No., Copyright (Year), with permission from Elsevier [OR APPLICABLE SOCIETY COPYRIGHT OWNER]." Also Lancet special credit - "Reprinted from The Lancet, Vol. number, Author(s), Title of article, Pages No., Copyright (Year), with permission from Elsevier."

4. Reproduction of this material is confined to the purpose and/or media for which permission is hereby given.

5. Altering/Modifying Material: Not Permitted. However figures and illustrations may be altered/adapted minimally to serve your work. Any other abbreviations, additions, deletions and/or any other alterations shall be made only with prior written authorization of Elsevier Ltd. (Please contact Elsevier at permissions@elsevier.com)

6. If the permission fee for the requested use of our material is waived in this instance, please be advised that your future requests for Elsevier materials may attract a fee.

7. Reservation of Rights: Publisher reserves all rights not specifically granted in the combination of (i) the license details provided by you and accepted in the course of this licensing transaction, (ii) these terms and conditions and (iii) CCC's Billing and Payment terms and conditions.

8. License Contingent Upon Payment: While you may exercise the rights licensed immediately upon issuance of the license at the end of the licensing process for the transaction, provided that you have disclosed complete and accurate details of your proposed use, no license is finally effective unless and until full payment is received from you (either by publisher or by CCC) as provided in CCC's Billing and Payment terms and conditions. If full payment is not received on a timely basis, then any license preliminarily granted shall be deemed automatically revoked and shall be void as if never granted. Further, in the event that you breach any of these terms and conditions or any of CCC's Billing and Payment terms and conditions, the license is automatically revoked and shall be void as if never granted. Use of materials as described in a revoked license, as well as any use of the materials beyond the scope of an unrevoked license, may constitute copyright infringement and publisher reserves the right to take any and all action to protect its copyright in the materials.

9. Warranties: Publisher makes no representations or warranties with respect to the licensed material.

10. Indemnity: You hereby indemnify and agree to hold harmless publisher and CCC, and their respective officers, directors, employees and agents, from and against any and all claims arising out of your use of the licensed material other than as specifically authorized pursuant to this license.

11. No Transfer of License: This license is personal to you and may not be sublicensed, assigned, or transferred by you to any other person without publisher's written permission.

12. No Amendment except in Writing: This license may not be amended except in writing signed by both parties (or, in the case of publisher, by CCC on publisher's behalf).

13. Objection to Contrary Terms: Publisher hereby objects to any terms contained in any purchase order, acknowledgment, check endorsement or other writing prepared by you, which terms are inconsistent with these terms and conditions or CCC's Billing and Payment terms and conditions. These terms and conditions, together with CCC's Billing and Payment terms and conditions (which are incorporated herein), comprise the entire agreement between you and publisher (and CCC) concerning this licensing transaction. In the event of any conflict between your obligations established by these terms and conditions and those established by CCC's Billing and Payment terms and conditions, these terms and conditions shall control.

14. Revocation: Elsevier or Copyright Clearance Center may deny the permissions described in this License at their sole discretion, for any reason or no reason, with a full refund payable to you. Notice of such denial will be made using the contact information provided by you. Failure to receive such notice will not alter or invalidate the denial. In no event will Elsevier or Copyright Clearance Center be responsible or liable for any costs, expenses or damage incurred by you as a result of a denial of your permission request, other than a refund of the amount(s) paid by you to Elsevier and/or Copyright Clearance Center for denied permissions.

LIMITED LICENSE

The following terms and conditions apply only to specific license types:

15. **Translation**: This permission is granted for non-exclusive world **English** rights only unless your license was granted for translation rights. If you licensed translation rights you

may only translate this content into the languages you requested. A professional translator must perform all translations and reproduce the content word for word preserving the integrity of the article. If this license is to re-use 1 or 2 figures then permission is granted for non-exclusive world rights in all languages.

16. **Posting licensed content on any Website**: The following terms and conditions apply as follows: Licensing material from an Elsevier journal: All content posted to the web site must maintain the copyright information line on the bottom of each image; A hyper-text must be included to the Homepage of the journal from which you are licensing at

http://www.sciencedirect.com/science/journal/xxxxx or the Elsevier homepage for books at

http://www.elsevier.com; Central Storage: This license does not include permission for a scanned version of the material to be stored in a central repository such as that provided by Heron/XanEdu.

Licensing material from an Elsevier book: A hyper-text link must be included to the Elsevier homepage at http://www.elsevier.com . All content posted to the web site must maintain the copyright information line on the bottom of each image.

Posting licensed content on Electronic reserve: In addition to the above the following clauses are applicable: The web site must be password-protected and made available only to bonafide students registered on a relevant course. This permission is granted for 1 year only. You may obtain a new license for future website posting.

For journal authors: the following clauses are applicable in addition to the above:

Permission granted is limited to the author accepted manuscript version* of your paper.

*Accepted Author Manuscript (AAM) Definition: An accepted author manuscript (AAM) is the author's version of the manuscript of an article that has been accepted for publication

and which may include any author-incorporated changes suggested through the processes of submission processing, peer review, and editor-author communications. AAMs do not include other publisher value-added contributions such as copy-editing, formatting, technical enhancements and (if relevant) pagination.

You are not allowed to download and post the published journal article (whether PDF or HTML, proof or final version), nor may you scan the printed edition to create an electronic version. A hyper-text must be included to the Homepage of the journal from which you are licensing at http://www.sciencedirect.com/science/journal/xxxxx. As part of our normal production process, you will receive an e-mail notice when your article appears on Elsevier's online service ScienceDirect (www.sciencedirect.com). That e-mail will include the article's Digital Object Identifier (DOI). This number provides the electronic link to the published article and should be included in the posting of your personal version. We ask that you wait until you receive this e-mail and have the DOI to do any posting.

Posting to a repository: Authors may post their AAM immediately to their employer's institutional repository for internal use only and may make their manuscript publically available after the journal-specific embargo period has ended.

Please also refer to Elsevier's Article Posting Policy for further information.

18. **For book authors** the following clauses are applicable in addition to the above:

Authors are permitted to place a brief summary of their work online only. You are not allowed to download and post the published electronic version of your chapter, nor may you scan the printed edition to create an electronic version. **Posting to a repository:** Authors are permitted to post a summary of their chapter only in their institution's repository.

20. **Thesis/Dissertation**: If your license is for use in a thesis/dissertation your thesis may be submitted to your institution in either print or electronic form. Should your thesis be published commercially, please reapply for permission. These requirements include permission for the Library and Archives of Canada to supply single copies, on demand, of the complete thesis and include permission for UMI to supply single copies, on demand, of the complete thesis. Should your thesis be published commercially, please reapply for permission.

Elsevier Open Access Terms and Conditions

Elsevier publishes Open Access articles in both its Open Access journals and via its Open Access articles option in subscription journals.

Authors publishing in an Open Access journal or who choose to make their article Open Access in an Elsevier subscription journal select one of the following Creative Commons user licenses, which define how a reader may reuse their work: Creative Commons Attribution License (CC BY), Creative Commons Attribution – Non Commercial - ShareAlike (CC BY NC SA) and Creative Commons Attribution – Non Commercial – No Derivatives (CC BY NC ND)

Terms & Conditions applicable to all Elsevier Open Access articles:

Any reuse of the article must not represent the author as endorsing the adaptation of the article nor should the article be modified in such a way as to damage the author's honour or reputation.

The author(s) must be appropriately credited.

If any part of the material to be used (for example, figures) has appeared in our publication with credit or acknowledgement to another source it is the responsibility of the user to ensure their reuse complies with the terms and conditions determined by the rights holder.

Additional Terms & Conditions applicable to each Creative Commons user license:

CC BY: You may distribute and copy the article, create extracts, abstracts, and other revised versions, adaptations or derivative works of or from an article (such as a translation), to include in a collective work (such as an anthology), to text or data mine the article, including for commercial purposes without permission from Elsevier

CC BY NC SA: For non-commercial purposes you may distribute and copy the article, create extracts, abstracts and other revised versions, adaptations or derivative works of or from an article (such as a translation), to include in a collective work (such as an anthology), to text and data mine the article and license new adaptations or creations under identical terms without permission from Elsevier

CC BY NC ND: For non-commercial purposes you may distribute and copy the article and include it in a collective work (such as an anthology), provided you do not alter or modify the article, without permission from Elsevier

Any commercial reuse of Open Access articles published with a CC BY NC SA or CC BY NC ND license requires permission from Elsevier and will be subject to a fee.

Commercial reuse includes:

· Promotional purposes (advertising or marketing)

· Commercial exploitation (e.g. a product for sale or loan)

· Systematic distribution (for a fee or free of charge)

Please refer to Elsevier's Open Access Policy for further information.

21. **Other Conditions**:

v1.6

You will be invoiced within 48 hours of this transaction date. You may pay your invoice by credit card upon receipt of the invoice for this transaction. Please follow instructions provided at that time.

To pay for this transaction now; please remit a copy of this document along with your payment. Payment should be in the form of a check or money order referencing your account number and this invoice number RLNK501364144.

Make payments to "COPYRIGHT CLEARANCE CENTER" and send to:

Copyright Clearance Center

Dept 001

P.O. Box 843006

Boston, MA 02284-3006

Please disregard electronic and mailed copies if you remit payment in advance.

Questions? customercare@copyright.com or +1-855-239-3415 (toll free in the US) or +1-978-646-2777.

Gratis licenses (referencing $0 in the Total field) are free. Please retain this printable

Appendix C

RE: Copyright permission request

pubscopyright [copyright@osa.org]

Sent:Tuesday, July 29, 2014 1:17 PM

To: Vivek Labhishetty

Dear Vivek Labhishetty,

Thank you for contacting The Optical Society. OSA considers your requested use of its copyrighted material to be Fair Use under United States Copyright Law. It is requested that a complete citation of the original material be included in any publication.

Let me know if you have any questions.

Kind Regards,

Susannah Lehman
July 29, 2014
Authorized Agent, The Optical Society

From: Vivek Labhishetty [mailto:vivek.labhishetty@uwaterloo.ca]

Sent: Tuesday, July 29, 2014 11:15 AM

To: pubscopyright

Subject: Copyright permission request

Dear Sir/Madam,

I would like to use two images in my thesis from an article by Austin Roorda and Melanie C.W. Campbell - "Slope based eccentric photorefraction: theoretical analysis of different light source configurations and effects of ocular aberrations" that was published in your journal (Journal of Optical society of America A, optics, image science and vision, Volume 14, No.

10, October 1997; Page number - 2547-2556). Kindly grant me permission to use the two images (Figure 4; Figure 8) from this article in my thesis,

Thank you in advance,

Regards,

Vivek

Appendix D

RE: Copyright permission request

Suryakumar, Rajaraman [rajaraman.suryakumar@alcon.com]

Sent:Wednesday, July 30, 2014 12:27 PM

To: Vivek Labhishetty

Vivek,

Certainly, please go ahead and use it.

Best regards,

Raj

From: Vivek Labhishetty [mailto:vivek.labhishetty@uwaterloo.ca]

Sent: Wednesday, July 30, 2014 10:44 AM

To: Suryakumar, Rajaraman

Subject: Copyright permission request

Dear Raj,

I am Vivek working with Dr.Bobier at University of Waterloo and hope you still remember me. Last time we spoke was a year ago about the Dynamic photorefraction system that you had worked on. I am about to finish up my thesis writing and complete my Masters successfully. I want to include a picture in your thesis (Study of the dynamic interactions between vergence and accommodation, 2005) that shows the difference in the velocity and acceleration profiles of accommodation obtained from a photorefractor working at 25Hz and 75Hz sampling frequency into my Master's thesis. Please provide a permission acceptance response so that i can include it in my thesis,

Thank you in advance,

Vivek

References

Chapter 1 Eccentric photorefraction

1. Atchison DA, Smith G. Chromatic dispersions of the ocular media of human eyes. J. Opt. Soc. Am. A. 2005;22(1):29-37.

2. Bharadwaj SR, Sravani NG, Little J, et al. Empirical variability in the calibration of slope-based eccentric photorefraction. J. Opt. Soc. Am. A. 2013;30(5):923-931.

3. Blade PJ, Candy TR. Validation of the PowerRefractor for measuring human infant refraction. Optom Vis Sci. 2006;83(6):346-353.

4. Bobier WR, Braddick OJ. Eccentric photorefraction: Optical analysis and empirical measures. Am J Optom Physiol Opt. 1985;62(9):614-620.

5. Choi M, Weiss S, Schaeffel F, et al. Laboratory, clinical, and kindergarten test of a new eccentric infrared photorefractor (PowerRefractor). Optom Vis Sci. 2000;77(10):537-548.

6. Ciuffreda KJ, Vasudevan B. Nearwork-induced transient myopia (NITM) and permanent myopia–is there a link? Ophthalmic Physiol Opt. 2008;28(2):103-114.

7. Curtin B, Whitmor W. The optics of myopia. Duane's Clinical Ophthalmology.Philadelphia: JB Lippincott. 1993.

8. Gwiazda J, Bauer J, Thorn F, Held R. A dynamic relationship between myopia and blur-driven accommodation in school-aged children. Vision Res. 1995;35(9):1299-1304.

9. Gwiazda J, Grice K, Thorn F. Response AC/A ratios are elevated in myopic children. Ophthalmic Physiol Opt. 1999;19(2):173-179.

10. Gwiazda J, Thorn F, Bauer J, Held R. Myopic children show insufficient accommodative response to blur. Invest Ophthalmol Vis Sci. 1993;34(3):690-694.

11. Howland HC. Photorefraction of eyes: History and future prospects. Optom Vis Sci. 2009;86(6):603-606.

12. Howland HC. Optics of photoretinoscopy: Results from ray tracing. Am J Optom Physiol Opt. 1985;62(9):621-625.

13. Hung GK. Adaptation model of accommodation and vergence. Ophthalmic Physiol Opt. 1992;12(3):319-326.

14. Jiang B, White JM. Effect of accommodative adaptation on static and dynamic accommodation in emmetropia and late-onset myopia. Optom Vis Sci. 1999;76(5):295-302.

15. Jiang B. Accommodative vergence is driven by the phasic component of the accommodative controller. Vision Res. 1996;36(1):97-102.

16. Millodot M, Bobier C. The state of accommodation during the measurement of axial chromatic aberration of the eye. Am J Optom Physiol Opt. 1976;53(4):168-172.

17. Morgan IG, Ohno-Matsui K, Saw S. Myopia. The Lancet. 2012;379(9827):1739-1748.

18. Mutti DO, Jones LA, Moeschberger ML, Zadnik K. AC/A ratio, age, and refractive error in children. Invest Ophthalmol Vis Sci. 2000;41(9):2469-2478.

19. Mutti DO, Mitchell GL, Hayes JR, et al. Accommodative lag before and after the onset of myopia. Invest Ophthalmol Vis Sci. 2006;47(3):837-846.

20. Roorda A, Campbell MC, Bobier WR. Slope-based eccentric photorefraction: Theoretical analysis of different light source configurations and effects of ocular aberrations. J. Opt. Soc. Am. A. 1997;14(10):2547-2556.

21. Roorda A, Campbell MC, Bobier W. Geometrical theory to predict eccentric photorefraction intensity profiles in the human eye. J. Opt. Soc. Am. A. 1995;12(8):1647-1656.

22. Schaeffel F, Wilhelm H, Zrenner E. Inter-individual variability in the dynamics of natural accommodation in humans: Relation to age and refractive errors. J Physiol. 1993;461(1):301-320.

23. Schaeffel F, Farkas L, Howland HC. Infrared photoretinoscope. Appl Opt. 1987;26(8):1505-1509.

24. Schaeffel F, Hagel G, Eikermann J, Collett T. Lower-field myopia and astigmatism in amphibians and chickens. J. Opt. Soc. Am. A. 1994;11(2):487-495.

25. Schor CM, Ciuffreda KJ. Vergence eye movements: Basic and clinical aspects. Butterworths Boston; 1983.

26. Schor CM, Kotulak JC. Dynamic interactions between accommodation and convergence are velocity sensitive. Vision Res. 1986;26(6):927-942.

27. Schor CM. The glenn A. fry award lecture: Adaptive regulation of accommodative vergence and vergence accommodation. Am J Optom Physiol Opt. 1986;63(8):587-609.

28. Sivak J. The cause (s) of myopia and the efforts that have been made to prevent it. Clin. Exp. Optom. 2012;95(6):572-582.

29. Sreenivasan V, Irving EL, Bobier WR. Effect of near adds on the variability of accommodative response in myopic children. Ophthalmic Physiol Opt. 2011;31(2):145-154.

30. Suryakumar R. Study of the dynamic interactions between vergence and accommodation. Collections Canada, 2005.

31. Suryakumar R, Kwok D, Fernandez S, Bobier WR. Dynamic photorefraction system: An offline application for the dynamic analysis of ocular focus and pupil size from photorefraction images. Comput Biol Med. 2009;39(3):195-205.

Chapter 2 Calibration of the DPRS

1. ACGIH. 2013 TLVs® and BEIs®: Threshold limit values for chemical substances and physical agents. 2013.

2. Blade PJ, Candy TR. Validation of the PowerRefractor for measuring human infant refraction. Optom Vis Sci. 2006;83(6):346-353.

3. Bobier WR, Braddick OJ. Eccentric photorefraction: Optical analysis and empirical measures. Am J Optom Physiol Opt. 1985;62(9):614-620.

4. Choi M, Weiss S, Schaeffel F, et al. Laboratory, clinical, and kindergarten test of a new eccentric infrared photorefractor (PowerRefractor). Optom Vis Sci. 2000;77(10):537-548.

5. Roorda A, Campbell MC, Bobier WR. Slope-based eccentric photorefraction: Theoretical analysis of different light source configurations and effects of ocular aberrations. J. Opt. Soc. Am. A. 1997;14(10):2547-2556.

6. Schaeffel F, Wilhelm H, Zrenner E. Inter-individual variability in the dynamics of natural accommodation in humans: Relation to age and refractive errors. J Physiol. 1993;461(1):301-320.

7. Schaeffel F, Farkas L, Howland HC. Infrared photoretinoscope. Appl Opt. 1987;26(8):1505-1509.

8. Schaeffel F, Hagel G, Eikermann J, Collett T. Lower-field myopia and astigmatism in amphibians and chickens. J. Opt. Soc. Am. A. 1994;11(2):487-495.

9. Suryakumar R. Study of the dynamic interactions between vergence and accommodation. Collections Canada, 2005.

10. Suryakumar R, Kwok D, Fernandez S, Bobier WR. Dynamic photorefraction system: An offline application for the dynamic analysis of ocular focus and pupil size from photorefraction images. Comput Biol Med. 2009;39(3):195-205.

Chapter 3 Validation of the DPRS

1. Adler FH, Kaufman PL, Levin LA, Alm A. Adler's physiology of the eye. Elsevier Health Sciences; 2011.

2. Alvarez TL, Semmlow JL, Yuan W, Munoz P. Dynamic details of disparity convergence eye movements. Ann Biomed Eng. 1999;27(3):380-390.

3. Atchison DA, Bradley A, Thibos LN, Smith G. Useful variations of the badal optometer. .Optom Vis Sci. 1995;72(4):279-284.

4. Bahill AT, Clark MR, Stark L. The main sequence, a tool for studying human eye movements. Math Biosci. 1975;24(3):191-204.

5. Baker DH, Meese TS, Mansouri B, Hess RF. Binocular summation of contrast remains intact in strabismic amblyopia. Invest Ophthalmol Vis Sci. 2007;48(11):5332-5338.

6. Bharadwaj SR, Schor CM. Acceleration characteristics of human ocular accommodation. Vision Res. 2005;45(1):17-28.

7. Blade PJ, Candy TR. Validation of the PowerRefractor for measuring human infant refraction. Optom Vis Sci. 2006;83(6):346-353.

8. Campbell FW, Westheimer G. Dynamics of accommodation responses of the human eye. J Physiol. 1960;151:285-295.

9. Choi M, Weiss S, Schaeffel F, et al. Laboratory, clinical, and kindergarten test of a new eccentric infrared photorefractor (PowerRefractor). .Optom Vis Sci. 2000;77(10):537-548.

10. Ciuffreda K, Kenyon R. Accommodative vergence and accommodation in normals, amblyopes, and strabismics. Vergence eye movements: basic and clinical aspects. Boston: Butterworths. 1983:101-173.

11. Fincham EF. The mechanism of accommodation. G. Pulman & sons, Limited; 1937.

12. Fincham EF. The accommodation reflex and its stimulus. Br J Ophthalmol. 1951;35(7):381-393.

13. Hartridge H. Helmholtz's theory of accommodation. Br J Ophthalmol. 1925;9(10):521-523.

14. Heath GG. Components of accommodation. Am J Optom Arch Am Acad Optom. 1956;33(11):569-579.

15. Heron G, Winn B. Binocular accommodation reaction and response times for normal observers. Ophthalmic Physiol Opt. 1989;9(2):176-183.

16. Hokoda S, Ciuffreda K. Theoretical and clinical importance of proximal vergence and accommodation. Vergence eye movements: basic and clinical aspects. 1983:75-97.

17. Hung GK. Dynamic model of the vergence eye movement system: Simulations using MATLAB/SIMULINK. Comput Methods Programs Biomed. 1998;55(1):59-68.

18. Hung GK. Adaptation model of accommodation and vergence. Ophthalmic Physiol Opt. 1992;12(3):319-326.

19. Hung GK, Semmlow JL. Static behavior of accommodation and vergence: Computer simulation of an interactive dual-feedback system. IEEE Trans Biomed Eng. 1980(8):439-447.

20. Kasthurirangan S, Vilupuru AS, Glasser A. Amplitude dependent accommodative dynamics in humans. Vision Res. 2003;43(27):2945-2956.

21. Kasthurirangan S, Glasser A. Influence of amplitude and starting point on accommodative dynamics in humans. Invest Ophthalmol Vis Sci. 2005;46(9):3463-3472.

22. Kent PR. Convergence accommodation. Am J Optom Arch Am Acad Optom. 1958;35(8):393-406.

23. Mansouri B, Thompson B, Hess R. Measurement of suprathreshold binocular interactions in amblyopia. Vision Res. 2008;48(28):2775-2784.

24. Maxwell J, Tong J, Schor CM. The first and second order dynamics of accommodative convergence and disparity convergence. Vision Res. 2010;50(17):1728-1739.

25. McLin LN,Jr, Schor CM. Voluntary effort as a stimulus to accommodation and vergence. Invest Ophthalmol Vis Sci. 1988;29(11):1739-1746.

26. Meese TS, Georgeson MA, Baker DH. Binocular contrast vision at and above threshold. J Vis. 2006;6(11):1224-1243.

27. Mordi J, Tucker J, Charman W. Effects of 0.1% cyclopentolate or 10% phenylephrine on pupil diameter and accommodation. Ophthalmic Physiol Opt. 1986;6(2):221-227.

28. Mordi JA, Ciuffreda KJ. Dynamic aspects of accommodation: Age and presbyopia. Vision Res. 2004;44(6):591-601.

29. Mordi JA, Lyle WM, Mousa GY. Effect of phenylephrine on accommodation. Am J Optom Physiol Opt. 1986;63(4):294-297.

30. Morgan MW. Accommodation and vergence. Am J Optom Arch Am Acad Optom. 1968;45(7):417-454.

31. Ogle KN, Schwartz JT. Depth of focus of the human eye. J. Opt. Soc. Am. A. 1959;49(3):273-279.

32. Phillips S, Stark L. Blur: A sufficient accommodative stimulus. Doc Ophthalmol. 1977;43(1):65-89.

33. Phillips S, Shirachi D, Stark L. Analysis of accommodative response times using histogram information. Am J Optom Arch Am Acad Optom. 1972;49(5):389-400.

34. Roorda A, Campbell MC, Bobier WR. Slope-based eccentric photorefraction: Theoretical analysis of different light source configurations and effects of ocular aberrations. J. Opt. Soc. Am. A. 1997;14(10):2547-2556.

35. Rosenfield M, Gilmartin B. Effect of target proximity on the open-loop accommodative response. Optom Vis Sci. 1990;67(2):74-79.

36. Sarkar S, Hasnat AM, Bharadwaj SR. Revisiting the impact of phenylephrine hydrochloride on static and dynamic accommodation. Indian J Ophthalmol. 2012;60(6):503-509.

37. Schaeffel F, Wilhelm H, Zrenner E. Inter-individual variability in the dynamics of natural accommodation in humans: Relation to age and refractive errors. J Physiol. 1993;461(1):301-320.

38. Schor CM. A dynamic model of cross-coupling between accommodation and convergence: Simulations of step and frequency responses. Optom Vis Sci. 1992;69(4):258-269.

39. Schor CM, Bharadwaj SR. Pulse-step models of control strategies for dynamic ocular accommodation and disaccommodation. Vision Res. 2006;46(1):242-258.

40. Schor CM, Ciuffreda KJ. Vergence eye movements: Basic and clinical aspects. Vol 429. Butterworth Boston; 1983.

41. Schor CM, Lott LA, Pope D, Graham AD. Saccades reduce latency and increase velocity of ocular accommodation. Vision Res. 1999;39(22):3769-3795.

42. Schor C, Horner D. Adaptive disorders of accommodation and vergence in binocular dysfunction. Ophthalmic Physiol Opt. 1989;9(3):264-268.

43. Schor C, Bharadwaj S. A pulse-step model of accommodation dynamics. Conf Proc IEEE Eng Med Biol Soc. 2004;1:766-769.

44. Shirachi D, Liu J, Lee M, Jang J, Wong J, Stark L. Accommodation dynamics I. range nonlinearity. Am J Optom Physiol Opt. 1978;55(9):631-641.

45. Sreenivasan V, Irving EL, Bobier WR. Can current models of accommodation and vergence predict accommodative behavior in myopic children? Vision Res. 2014.

46. Sreenivasan V, Irving EL, Bobier WR. Effect of heterophoria type and myopia on accommodative and vergence responses during sustained near activity in children. Vision Res. 2012;57:9-17.

47. Stark L, Takahashi Y, Zames G. Nonlinear servoanalysis of human lens accommodation. IEEE Trans Syst Man Cybern. 1965;1(1):75-83.

48. Sun F, Stark L. Dynamics of accommodation: Measurements for clinical application. Exp Neurol. 1986;91(1):71-79.

49. Suryakumar R, Bobier W. Brightness profiles in eccentric photorefraction crescents. Invest Ophthalmol Vis Sci. 2002;43(12):2670.

50. Suryakumar R. Study of the dynamic interactions between vergence and accommodation. Collections Canada, 2005.

51. Suryakumar R, Kwok D, Fernandez S, Bobier WR. Dynamic photorefraction system: An offline application for the dynamic analysis of ocular focus and pupil size from photorefraction images. Comput Biol Med. 2009;39(3):195-205.

52. Suryakumar R, Meyers JP, Irving EL, Bobier WR. Vergence accommodation and monocular closed loop blur accommodation have similar dynamic characteristics. Vision Res. 2007;47(3):327-337.

53. Tucker J, Charman WN. Reaction and response times for accommodation. Am J Optom Physiol Opt. 1979;56(8):490-503.

54. Ward P, Charman W. Effect of pupil size on steady state accommodation. Vision Res. 1985;25(9):1317-1326.